



Short-term variation of pH in seawaters around coastal areas of Japan: Characteristics and forcings

5 Tsuneo Ono¹, Daisuke Muraoka², Masahiro Hayashi³, Makiko Yorifuji^{3*}, Akihiro Dazai⁴, Shigeyuki Omoto⁵, Takehiro Tanaka⁶, Tomohiro Okamura⁷, Goh Onitsuka⁷, Kenji Sudo⁷, Masahiko Fujii^{8#}, Ryuji Hamanoue⁸, and Masahide Wakita⁹

¹Fisheries Resources Institute, Japan Fisheries Research and Education Agency, Yokohama, 236-8648, Japan

²Fisheries Technology Institute, Japan Fisheries Research and Education Agency, Miyako, 027-0097, Japan

³Marine Ecology Research Institute, Kashiwazaki, 945-0017, Japan

⁴Center for Sustainable Society, Minami-Sanriku, 986-0775, Japan

10 ⁵Eight-Japan Engineering Consultants Inc., Okayama, 700-8617, Japan

⁶Satoumi Research Institute, Okayama, 704-8194, Japan

⁷Fisheries Technology Institute, Japan Fisheries Research and Education Agency, Hatsukaichi, 739-0452, Japan

⁸Faculty of Environmental Earth Science, Hokkaido University, Sapporo, 060-0810, Japan

⁹Mutsu Institute for Oceanography, Japan Agency for Marine-Earth Science and Technology, Mutsu, 035-0022, Japan

15 *now at National Institute of Advanced Industrial Science and Technology, Tsukuba, 305-8560, Japan

#now at Otsuchi Coastal Research Center, Atmosphere and Ocean Research Institute, the University of Tokyo, Otsuchi, 028-1102, Japan

Correspondence to: Tsuneo Ono (tono@fra.affrc.go.jp)

Abstract. The pH of coastal seawater varies based on several local forcings, such as water circulation, terrestrial inputs, and biological processes, and these forcings can change along with global climate change. Understanding the mechanism of pH variation in each coastal area is thus important for a realistic future projection that considers changes in these forcings. From 2020 to 2021, we performed parallel year-round observations of pH and related ocean parameters at five stations around the Japanese coast (Miyako Bay, Shizugawa Bay, Kashiwazaki Coast, Hinase Archipelago, and Ohno Strait) to understand the characteristics of short-term pH variations and their forcings. Annual variability (~1 standard deviation) of pH and aragonite saturation state (Ω_{ara}) were 0.05–0.09 and 0.25–0.29, respectively, for three areas with low anthropogenic loadings (Miyako Bay, Kashiwazaki Coast, and Shizugawa Bay), while it increased to 0.16–0.21 and 0.52–0.58, respectively, in two areas with medium anthropogenic loadings (Hinase Archipelago and Ohno Strait in Seto Inland Sea). Statistical assessment of temporal variability at various timescales revealed that most of the annual variabilities in both pH and Ω_{ara} were derived by short-term variation at a timescale of < 10 days, rather than seasonal-scale variation. Our analyses further illustrated that most of the short-term pH variation was caused by biological processes, while both thermodynamic and biological processes equally contributed to the temporal variation in Ω_{ara} . The observed results showed that short-term acidification with $\Omega_{\text{ara}} < 1.5$ occurred occasionally in Miyako and Shizugawa Bays, while it occurred frequently in the Hinase Archipelago and Ohno Strait. Most of such short-term acidified events were related to short-term low-salinity events. Our analyses showed that the amplitude of short-term pH variation was linearly correlated with that of short-term salinity variation, and its regression coefficient at the



35 time of high freshwater input was positively correlated with the nutrient concentration of the main river that flows into the coastal area.

1 Introduction

The ocean is lowering its pH because of anthropogenic CO₂ input both in open (e.g., Bates et al., 2014; Iida et al., 2021; Jiang et al., 2019; Lauvset et al., 2015; Takahashi et al., 2014) and coastal oceans (e.g., Carstensen and Duarte, 2019; Duarte et al., 2013; Hauri et al., 2013; Ishizu et al., 2019; Ishida et al., 2021; Yao et al., 2022). In the coastal ocean, pH also showed short time variation caused by several processes such as water mass change (e.g., Johnson et al., 2013; Ko et al., 2016; Wakita et al., 2021), coastal upwelling (e.g., Barton et al., 2012; Booth et al., 2012; Feely et al., 2008, 2016; Vargas et al., 2015), input of river water (e.g., Cai et al., 2017; Fujii et al., 2021; Gomez et al., 2021; Salisbury and Jönsson, 2018; Salisbury et al., 2008), terrestrial nutrient input (e.g., Cai et al., 2011; Guo et al., 2021; Kessouri et al., 2021; Provoost et al., 2010; Sunda and Cai, 2012; Wallace et al., 2014), and various coastal biological processes (e.g., Delille et al., 2009; Mongin et al., 2016; Lowe et al., 2019; Ricart et al., 2021; Yamamoto-Kawai et al., 2021). The amplitude of short-term pH variation often exceeds that of the decadal-scale long-term pH trend, and hence, blurs the signal of anthropogenic CO₂-induced acidification of coastal seawater (e.g., Borges and Gypens, 2010; Duarte et al., 2013, Johnson et al., 2013; Provoost et al., 2010; Salisbury and Jönsson, 2018). Short-term pH variation in coastal waters is also important for local ecosystems because most coastal short-term pH variations are caused by natural forcings that have been acting from pre-industrial periods, and hence, the local ecosystem is expected to adapt to such short-term pH variations with natural timing and amplitude. For example, *Ostrea lurida*, a native oyster in Netarts Bay, Oregon, USA, has adjusted its spawning season before and after the summer upwelling season so that its larvae can avoid low-pH waters (Waldbusser et al., 2014). Several anthropogenic perturbations, such as change in land use, sewerage treatment, vanishment of seagrass bed, and modification of coastal topography, can change these forcings, shifting the timing and/or amplitude of natural short-term pH variation (e.g., Papalexiou and Montanari, 2019; Hoshiba et al., 2021). Understanding the present situation as well as the mechanism of short-term pH variation in coastal waters is thus critical for evaluating the risk of acidification in coastal areas.

Japan consists of 14,125 islands distributed in a wide latitudinal range from 20 °N to 45 °N in the western North Pacific, containing diverse coastal environments from coral reefs to seasonal floating sea ice. Japan is a highly developed country, and a significant portion of its coastal area has experienced various types of anthropogenic perturbations. The Japan Ministry of the Environment (MOE) conducts regular pH monitoring at over 2,000 coastal stations around Japan from the early 1980s until the present, and the obtained data showed significant variability in the multi-decadal pH trend from -0.012 y^{-1} to $+0.009 \text{ y}^{-1}$ among the stations (Ishizu et al., 2019). The observed range of pH trend within the Japanese coast corresponds to 85% of that observed in 83 coastal systems in the world (Carstensen and Duarte, 2019), and this result suggests that the Japanese coastal area can function as the “sample shelf” of the coastal environment for the entire world. The MOE monitors



pH monthly and seasonally, and several of pH stations of MOE, especially those in northern areas, lack wintertime observations (Ishizu et al., 2019). We thus need additional pH observations with a higher time resolution to understand the characteristics of short-term pH variation at a timescale of < 30 days around the Japanese coast to assess its variability and mechanisms. A number of scientists have already started such pH monitoring in coastal stations in Japan (e.g., Christian and Ono, 2019; Fujii et al., 2021, 2023; Ishida et al., 2021; Wakita et al., 2021). However, most of these observations were started recently and the summarisation of observed results among these stations is yet to be made. In this study, we summarised continuous monitoring data of pH observed during 2020–2021 at five stations around the Japanese coast. In this study, we describe and discuss the amplitude of pH variation in each timescale, similarity, and dissimilarity in the characteristics of variation, and their forcings.

75 2 Observations and settings of study areas



Figure 1: Map of the five study stations along the coast of Japan.

Hydrographic monitoring, including pH monitoring, was performed at five stations around the coast of Japan, Miyako Bay, Shizugawa Bay, Kashiwazaki Coast, Hinase Archipelago, and Ohno Strait (Fig. 1), from 2020 to 2021. The detailed settings of the areas and observation procedures are described in the following sections.

2.1 Miyako Bay

Miyako Bay is located in the northern part of Honshu Island facing the western North Pacific, with a bay area of 24 km² and 4.8-km wide bay mouth (Fig. 2(a)). The outer bay area is usually occupied by temperate western North Pacific water, which brings enough nutrients in winter to support seaweed farms in the coastal area (Kakehi et al., 2018). Additional nutrients to the bay are provided by three rivers, Hei, Tsugaruishi, and Tashiro Rivers (25.8, 5.16, and 3.78 m³ s⁻¹, respectively, for

annual average flow rate, Okada et al., 2014), although the quantity of nutrient input by the rivers are limited to low levels (57, 11, and 8 tN y⁻¹ for Hei, Tsugaruishi, and Tashiro Rivers, respectively, Bernardo et al., 2023). With a population of 60,000 within the hinterland, Miyako Bay has maintained good water quality with 1–2 mg L⁻¹ of chemical oxygen demand (MOE,



95 2022). While kelp beds are well developed near the shoreline, wakame seaweed (*Undaria pinnatifida*) farmyards are developed in the middle of the bay.

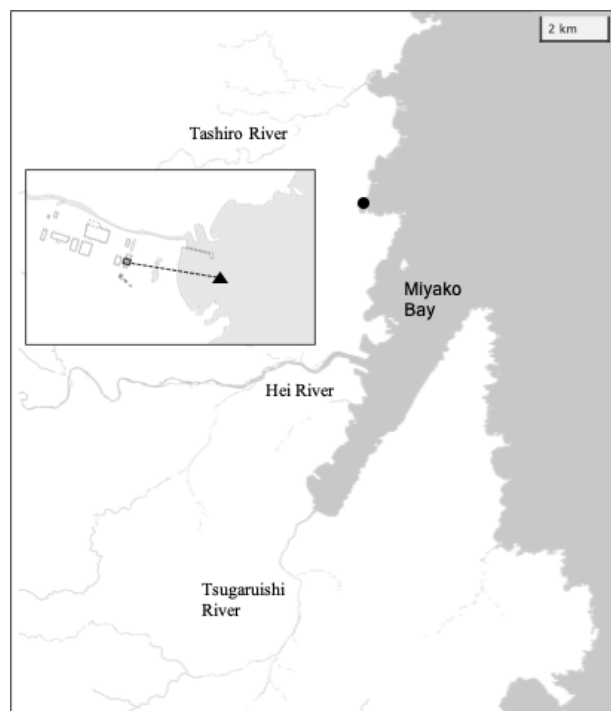


Figure 2: Map of Miyako Bay with the location of the station (solid circle). Overlaid map shows detailed structure of the station. Grey square and solid triangle represent locations of settling tank and water intake, respectively.

120 28181, respectively) at the beginning of each deployment. Along with these measurements, discrete water samples were taken from the tank at a depth of 1 m using a 1.5-L Niskin bottle every week. Subsamples for salinity, nutrients, dissolved inorganic carbon (DIC), and total alkalinity (Talk) were then taken and stored. Salinity and nutrients were measured at the Yokohama Laboratory of the Japan Fisheries Research and Education Agency using a salinometer (Guildline Instruments 8400 B) and continuous flow analyser (Seal Analytical QuAAtro 39), respectively, while DIC and Talk were measured at the Mutsu Institute for Oceanography of the Japan Agency for Marine-Earth Science and Technology (MIO-JAMSTEC) using a carbon coulometer (UIC CM 5012 with Nippon ANS MODEL 3000A) and an open-cell titrator (Kimoto Electric ATT-15) calibrated against the seawater reference materials provided by KANSO Corporation (Wakita et al., 2021). The pH of the seawater at the time of each sampling ($\text{pH}_{\text{discrete}}$) was calculated from DIC and Talk using the CO2sys program v2.1 (Lewis and Wallace 1998), with the settings of Lueker et al. (2000) for the dissociation constant of carbonate, Dickson (1990) for the dissociation constant

125

The monitoring site was located in front of the Miyako Field Station of the Japan Fisheries Research and Education Agency, which is located north of the bay mouth ($141^{\circ} 58' 5'' \text{ E}$ and $39^{\circ} 41' 28'' \text{ N}$; Fig 2(a)). This area frequently encounters severe winter storms, so we set the monitoring station in the settling tank ($3.6 \times 2.8 \times 5.4 \text{ m}$) of the field station, in which coastal water is continuously pumped from the water intake located 200 m off the coastline and 1–3 m in depth (Fig. 2(b)). Sensors for pH (Kimoto Electronic, SPS-14), dissolved oxygen (DO) (JFE Advantech, AROW2), and salinity/water temperature (JFE Advantech, ACTW) were then moored at a depth of 1 m in the settling tank. The difference in pH between water intake and settling tank was measured for two weeks during the monitoring period, and it was confirmed that the difference in pH between the water intake and settling tank was < 0.006 . The sampling frequency of each sensor was set to 1 h. All sensors were replaced every 2 months, and the DO sensor was calibrated by air-saturated pure water and sodium sulphite solution, while the pH sensor was calibrated against tris(hydroxymethyl)aminomethane and 2-amino-2-methyl-1-propanol-buffered artificial seawaters provided by FUJIFILM Wako Pure Chemical Corporation (Cat. No. 017-28191 and 010-



of bisulphate, and Lee et al. (2010) for the aqueous boron concentration. The drift of the pH sensor during deployment was corrected based on the difference between $\text{pH}_{\text{discrete}}$ and the pH measured by the sensor. The relationship between the measured
130 Talk and salinity was evaluated as a linear function, and the time series of Talk throughout the sensor deployment was
calculated based on the salinity–Talk relationship. The saturation states of calcite (Ω_{cal}) and aragonite (Ω_{ara}) were then
calculated from water temperature, salinity, nutrient concentrations, DIC, and Talk using the CO2sys program. This monitoring
program, founded by the Study Biological Effects of Acidification and Hypoxia (BEACH) of the Environment Research and
Technology Development Fund of the Environmental Restoration and Conservation Agency, which was started on 1 July 2020
135 and ended on 21 September 2021.

2.2 Kashiwazaki Coast

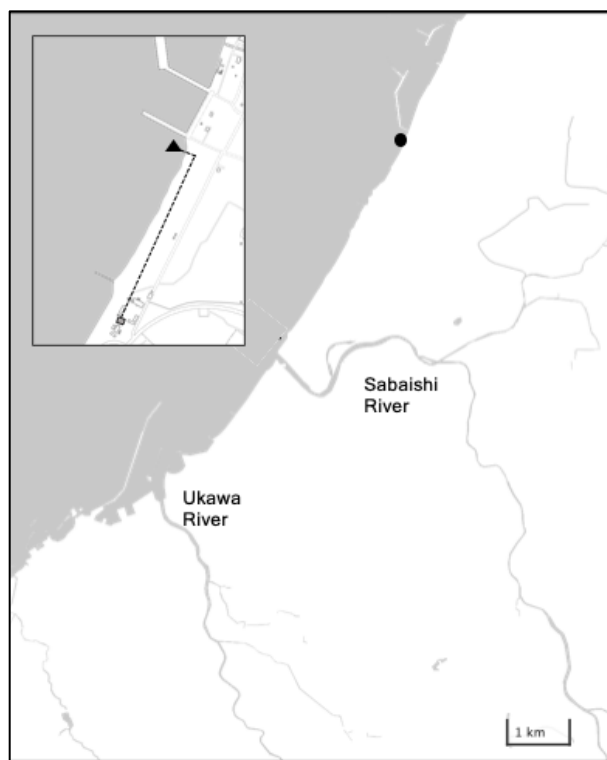


Figure 3: (a) Detailed map of Kashiwazaki Coast with the location of the station (solid circle). (b) Locations of water intake and settling tank in Kashiwazaki Observatory.

Kashiwazaki City is located at the centre of Honshu Island facing the Sea of Japan. Its coastline has little flexure, with the periodic occurrence of shallow sandy beaches and small rocky reefs (Fig. 3(a)). While benthic biomass is quite low in sandy beach coastal areas, local *Sargassum* seaweed beds are formed off rocky reefs. The low-nutrient Tsushima Warm Current flows throughout the year off the narrow band of low-salinity coastal water (Niigata Prefectural Institute for Fisheries and Oceanography, 1998). Kashiwazaki City has a population of 79,000 with a cultivated land area of 4,890 ha (mainly rice paddy fields) and ~200 plants of manufacturing industries. Sewage waters from these civil activities are released into coastal areas via two small rivers, Sabaishi and Ukawa Rivers, which bring low salinity and nutrients. The quality of off-Kashiwazaki coastal waters has been well maintained, with a chemical oxygen demand of $< 2 \text{ mg L}^{-1}$ (MOE, 2022). However, 30 years of monitoring by the Marine Ecology Research Institute shows that the pH of off-Kashiwazaki coastal water has decreased at a rate of -0.003 y^{-1} because of the increase in water temperature and concentration of atmospheric CO_2 (Ishida et al., 2021).

Similar to the Miyako site, sensors for pH, DO, and salinity/water temperature were set within the water tank (3,000 L), to which

coastal water was continuously pumped from the water intake set in front of the Marine Ecology Research Institute ($138^\circ 35'$



160 24" E and 37 °25' 30" N, Fig. 3(b)). The settings of each sensor, water sampling, and measurements were the same as those of the Miyako site. This monitoring program, also founded by BEACH, started on 16 July 2020 and ended on 24 August 2021.

2.3 Shizugawa Bay

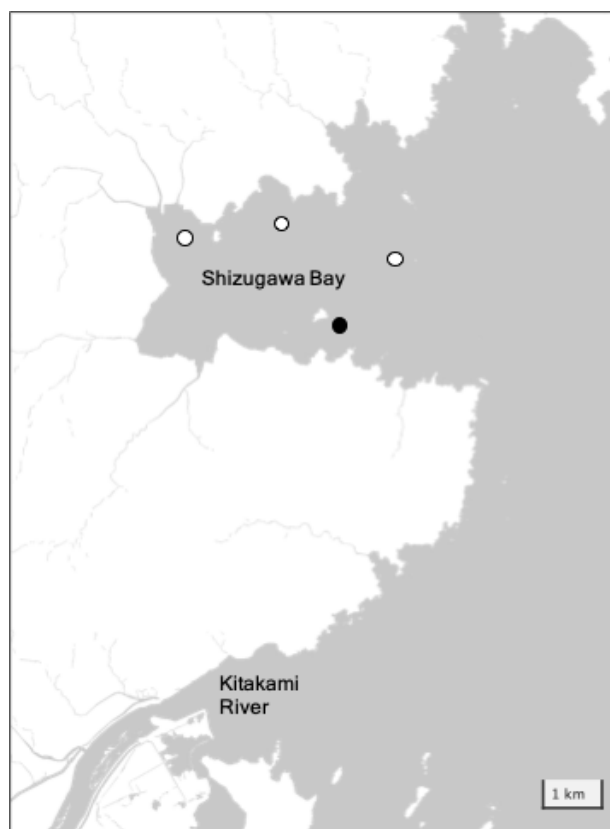


Figure 4: Detailed map of Shizugawa Bay with the location of the station. Open circles represent stations installed by the Ocean Acidification Adaptation Project. Solid circle represents the location of station S3 used in this study.

Shizugawa Bay is located ~100 km south of Miyako Bay, with a bay area of 46.8 km² and a 6.6-km wide bay mouth (Fig. 4). The Oyashio-oriented cold-water and Kuroshio-oriented warm-water masses intermittently occupy the outer bay, and the former water brings high quantities of nutrients to this bay in winter, similar to that in the Miyako Bay. The large Kitakami River (water transport of 390 m³ s⁻¹), flows out to the sea south of Shizugawa Bay, bringing nutrients of 6 × 10³ tN y⁻¹ to the coastal area (Sugimura et al., 2015). In addition, 10 small rivers flow directly into the bay, and the total nutrient flux provided by these rivers was estimated at 270 tN y⁻¹ (Yamamoto et al., 2018). Shizugawa Bay has been widely used for the aquaculture industry, especially for culturing Pacific oysters and silver salmon. Historically, the extent of aquaculture utilisation occasionally becomes too heavy, resulting in the emergence of low-oxygen deep waters in the bay caused by the degradation of organic materials derived from aquaculture. After the Great East Japan Earthquake in 2011, oyster farmers in Shizugawa Bay decided to reduce the numbers of their oyster rafts to one third of that they had before the earthquake to diminish the environmental impact of aquaculture on the bay ecosystem, which was on the way to recovery from the tsunami disaster. As a result, the DO of the bottom water in the bay showed a marked increase to > 1 mg L⁻¹ (Yamamoto et al., 2017).

190 Since 2020, hydrographic conditions, including pH, have been observed at four stations within Shizugawa Bay (Fig. 4) by the Ocean Acidification Adaptation Project (OAAP) founded by the Nippon Foundation (Fujii et al., 2023). Detailed settings of the observations are described in Fujii et al. (2023), and here, we reproduce its brief outline: Sensors for water temperature, salinity, DO, and pH were set at a depth of 1 m in each station to collect data at a temporal resolution of 1 h. Water samples for salinity, nutrients, DIC, and Talk were taken from each station monthly, and the sampling interval was



enhanced to every 15 days during summer. Salinity, nutrients, DIC, and Talk were measured by the same methods as for the Miyako site, although measurements were made at the Kesen-numa Laboratory of Miyagi Prefectural Institute for Fisheries Sciences and MIO-JAMSTEC for nutrients and other properties, respectively. Similar to the Miyako site, $\text{pH}_{\text{discrete}}$ was calculated from DIC and Talk and used for the drift correction of the pH sensors. The time series of Talk throughout the sensor deployment was also calculated based on the observed Talk–salinity relationship. In this study, we used data from Station S3 (Fig.4) as a representative of Shizugawa Bay, as this station is located in oyster farming areas, the largest aquaculture industry, which is the largest source of organic carbon in this bay. The measurement of water temperature, salinity, and pH was started on 20 August 2020, while that of DO on 27 April 2021. All parameters are continuously measured till date; however, we use data from August 2020 to December 2021 to maintain synchronicity with data of other stations.

2.4 Hinase Archipelago



Figure 5: Detailed map of Hinase Archipelago with the location of the station. Open circles represent stations installed by the Ocean Acidification Adaptation Project. Solid circle represents the location of station H2 used in this study.

The Seto Inland Sea is the largest inner sea in Japan (~23,200 km²) surrounded by the Honshu, Shikoku, and Kyushu Islands, and the Hinase Archipelago is located in the middle of the Seto Inland Sea. This area consists of four major waterways and many small canals divided by Honshu Island and eight other small islands with a water depth of ~6 m (Fig. 5). The Seto Inland Sea is a moderately eutrophicated area, receiving 53.0 km³ y⁻¹ of freshwater and 141,000 tN y⁻¹ of nitrate from the surrounding lands (Higashi et al., 2018; Nishijima, 2018). The water

exchange rate between the Seto Inland Sea and the outer North Pacific is also high (residence time of ~8 months, Yanagi and Ishii, 2004), and as a result, the nutrient concentration of surface water in the Seto Inland Sea is maintained at a moderate level (~0.4 μM of DIN near the Hinase Archipelago, Tsukamoto and Yanagi, 1998). Historically, nutrient loading was the highest in the 1980s (~235,000 tN y⁻¹, Nishijima, 2018). While the long-standing efforts of local communities succeeded in reducing it to the current level, significant quantities of organic nutrients still remained in the bottom sediment, creating local internal



225 sources of nutrients in the Seto Inland Sea (e.g., Yamamoto et al., 2021). Although there is no large point source of nutrients,
such as chemical plants, near the Hinase Archipelago, this area also receives nutrients from the Bizen city, that has a population
of 36,000. The Chikusa River, with an average flow rate of $33.5 \text{ m}^3 \text{ s}^{-1}$, flows in the eastern edge of this area, while several
other small streams provide additional freshwater. The coastal area of the southern Hinase Archipelago is filled with eelgrass
beds, while the northern coastal areas are partially filled with artificial shorelines, such as port facilities and breakwaters.
Oyster aquaculture is widely used in open-water areas. The OAAP also launched four stations in this area (Fig. 5). Settings of
230 sensors, water sampling, and its measurements were the same as those of Shizugawa Bay, with the exception that nutrient
measurements were done by the Okayama Prefectural Institute of Fisheries Sciences (see Fujii et al., 2023 for details). In this
study, we used data from Station H2 (Fig.5) to represent the Hinase Archipelago, as this station is located in the centre of
oyster farming areas. Measurements of water temperature, salinity, and pH were started on 29 August 2020, while
measurements of DO was started on 10 June 2021. All parameters are continuously measured till date; however, we use data
235 from August 2020 to December 2021.

2.5 Ohno Strait



Figure 6: Detailed map of Ohno Strait with the location of the station (solid circle).

Ohno Strait is the small strait between Honshu and Miyajima Islands, which are located at the southern boundary of Hiroshima Bay in the western Seto Inland Sea (Fig. 6). As part of the Seto Inland Sea, the surface water surrounding Ohno Strait is moderately eutrophicated ($\sim 2 \mu\text{M}$ of DIN; Tsukamoto and Yanagi, 1998), although it is slightly lower than the Hinase Archipelago, reflecting an east–west gradient of surface nutrient concentration. The Ohta River, which flows through Hiroshima city with a population of 1.2 million, adds $1,930 \text{ tN y}^{-1}$ of nitrogen into Hiroshima Bay (Yamamoto et al., 2002). Part of the Ohta River water plume flows into the Ohno Strait (Abo and Onitsuka, 2019), providing nutrients to the surface layer of this strait. Industrial areas with a population of 115,000 are developed along the western coast of this strait, providing another nutrient source to this area. The strait itself is

lightly used for oyster farming, and the bottom sediment in the strait is mainly filled by silt and shell fragments.

The monitoring station was launched in the experimental raft off the Hatsukaichi Field Station of the Japan Fisheries Research and Education Agency, with a water depth of 3–6 m depending on the tide. A set of sensors (Kimoto Electronic SPS-14 for
255 pH, JFE Advantech AROW2 for DO, and JFE Advantech ACTW for salinity/water temperature) were hung from the raft at a



depth of 1 m, and each parameter was measured at an interval of 1 h. The methods and frequencies for sensor calibration and discrete water sampling were the same as those of the Miyako site. This station was launched on 22 June 2021 by the OAAP and is continuing to operate till date; however, we used data from June 2021 to December 2021.

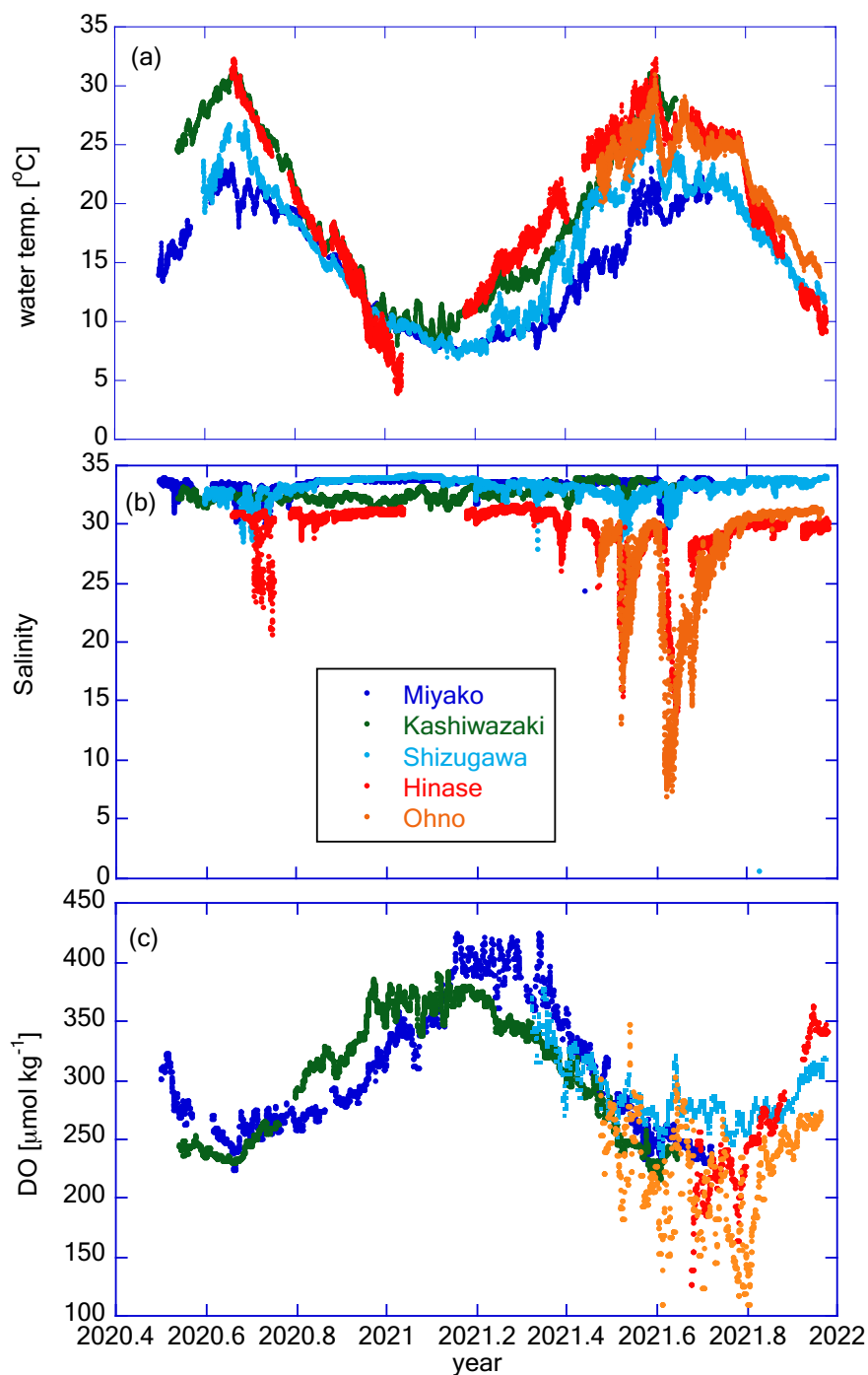
260 3 Results

3.1 Temporal variation of water temperature, salinity, and DO

Figure 7 shows the time series of water temperature, salinity, and DO at the five stations. All stations showed similar seasonal variations in water temperature, with the highest and lowest temperatures in July and February, respectively (Fig. 7(a)). The seasonal amplitude was the highest in Hinase and the lowest in Miyako. At all stations, water temperature showed significant day-to-day variation with a timescale of < 10 days, and also diurnal variations. We discuss this further in Section 4.1.

Time series of salinity in Shizugawa, Hinase, and Ohno show similar patterns of seasonal variation, low in summer/autumn and high in winter (Fig. 7(b)), suggesting that the main source of freshwater in these areas are rainfall events (during the rainy season in June/July and typhoon season in August–October). In contrast, in Kashiwazaki, salinity is high in summer and low in winter, suggesting that the main freshwater source in this area is snowfall in winter. The salinity of the Miyako site shows two low-salinity peaks, one in spring and the other in autumn, suggesting that this area is affected by both snowmelt waters and typhoon events. In Miyako, Shizugawa, Hinase, and Ohno, where the freshwater input is significant in summer/autumn, salinity frequently showed short-term drawdown that is synchronised with local rainfall events. The amplitude of sporadic salinity drawdown was extremely high in Hinase and Ohno, where the surface salinity temporarily reached < 10 (Fig. 7(b)). We discuss the effect of these short-term low salinity events on pH in Section 4.3.

DO showed similar patterns of seasonal variation: low in summer and high in winter, although the durations were short in Hinase and Ohno (Fig. 7 (c)). This pattern suggests that the seasonal variation of DO is mainly driven by variation of oxygen solubility induced by water temperature rather than biological processes. This seasonal variation overlaps with day-to-day variation with a duration of ~ 10 days, and the amplitude of such day-to-day variation is especially significant in Hinase and Ohno in summer and autumn. Because of this short-term day-to-day variation, DO in Hinase and Ohno were occasionally below $150 \mu\text{mol kg}^{-1}$ in summer and autumn, indicating that water conditions in these two areas occasionally become significantly undersaturated in DO, even in surface waters.



285 **Figure 7:** Time series of (a) water temperature, (b) salinity, and (c) DO in the five stations. Legends of colour plots are the same for all panels as shown in Fig. 7(b). In all graphs, the X-axis is expressed as year in decimal (e.g., 2021.2 = 36.5 days after Jan 1st 2021).



3.2 Temporal variation of pH

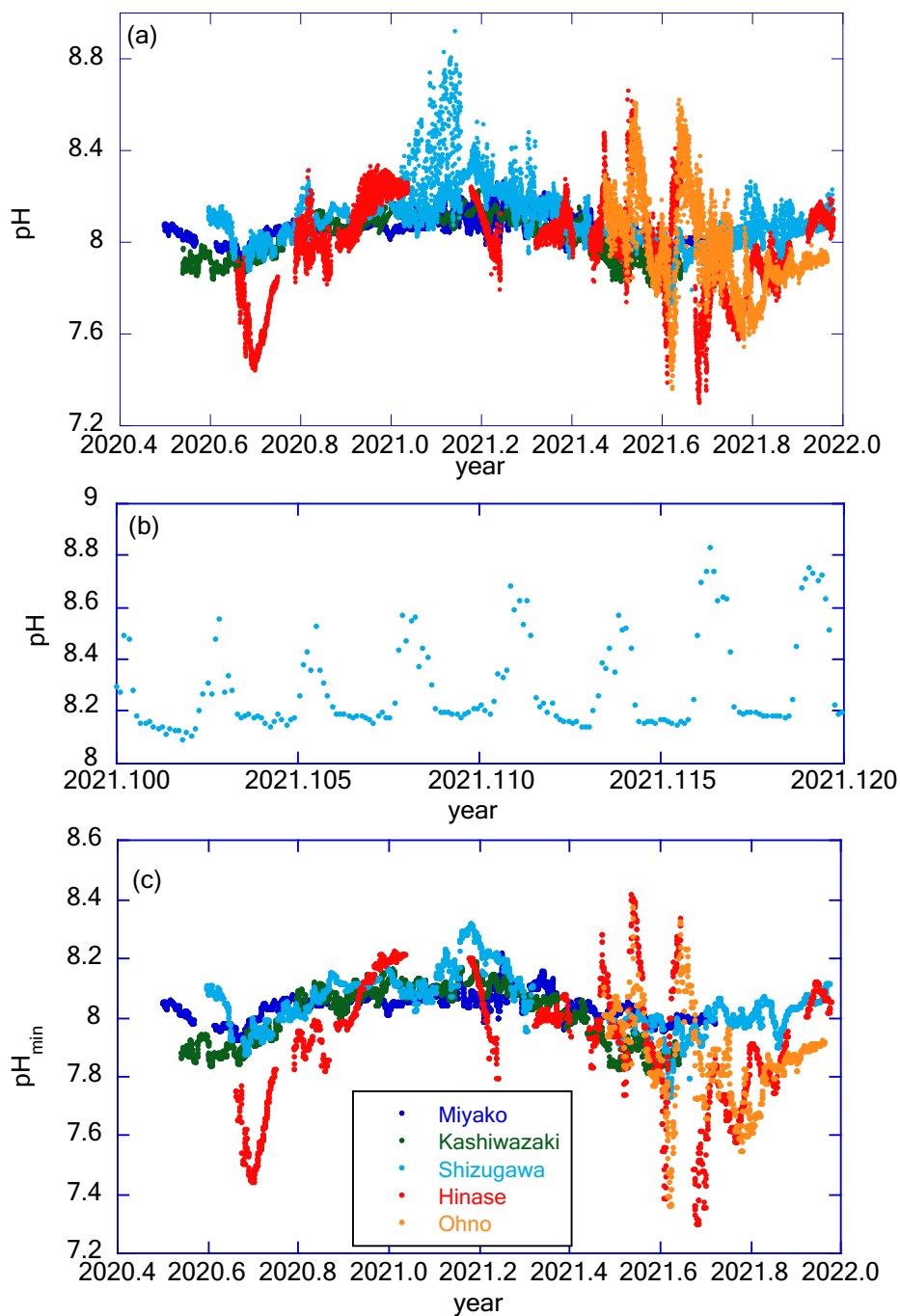
Figure 8(a) shows the time series of raw pH at five stations. Although the mechanistic precision of the pH sensor is ± 0.003 , the uncertainty of the pH value measured by the glass electrode is mainly controlled by the precision of its drift correction. In the case of Miyako, where drift correction was performed weekly, we set two pH sensors in the same settling tank for two weeks to evaluate the reliability of pH data after the drift correction process. Values of pH obtained from the two sensors matched with that of 2 standard deviation (SD) of ± 0.010 , and we used this value as the uncertainty of pH values obtained at Miyako, Kashiwazaki, and Ohno stations. In Shizugawa and Hinase, drift corrections were made at longer intervals, and Fujii et al. (2023) evaluated the uncertainty of pH at these two stations at ± 0.015 . Figure 8(a) shows significant daily fluctuations far higher than these pH uncertainties. The diurnal amplitude was the highest in winter in Shizugawa Bay, where the difference in pH between daytime and night-time exceeded 0.8. High diurnal variations in pH and/or $p\text{CO}_2$ are often measured in shallow coastal ecosystems (e.g., Waldbusser et al., 2014; Fujii et al., 2021; Ricart et al., 2021). In most cases, high diurnal pH variation is observed in summer, and the highest diurnal amplitude of pH in winter has rarely been reported. Such phenomena raise the possibility of biofouling in pH sensors, although visual inspection at the time of sensor exchange did not show significant adherence of biomes during winter. However, the detailed pH variation in each day (Fig. 8(b)) showed that during the night-time it was relatively low and constant, even during significant diurnal variation. This is probably because the organic material produced by the fouling biomes during daytime had settled down from the sensors, and hence, the effect of the decomposition of organic materials during night-time remained low even in the high diurnal variation period. We do not further discuss diurnal variations of pH, as we do not have definite evidence for the effect of biofouling in winter in Shizugawa Bay. We alternatively calculated the daily minimum pH (pH_{min}), that is usually observed at night, and analysed the day-to-day variation of pH_{min} at various timescales (Fig. 8(c)). Several rearing experiments have suggested that coastal organisms are affected by pH_{min} rather than the daily average pH (e.g., Onitsuka et al., 2018), therefore, the daily variation of pH_{min} was analysed instead of pH.

pH_{min} showed a similar pattern of seasonal variations at all five stations, with high values in winter and low values in summer/autumn (Fig. 8(c)). Seasonal amplitude was the lowest in Miyako and the highest in Hinase and Ohno (Fig. 7(a)). This seasonal variation overlapped with the short-term drawdown event of pH_{min} , which was frequently observed in summer/autumn. The timing of the amplitude of such events was synchronised with that of short-term low-salinity events (Fig. 7(b)). This phenomenon indicates that either rainfall or increased river flow causes several short-term processes in these coastal areas, causing short-term variation in pH.

315

3.3 Relationship between Talk and salinity

Figure 9 shows the observed relationship between Talk and salinity based on discrete water samples obtained at each station. Talk values in Miyako, Kashiwazaki, and Shizugawa converged into a narrow range 2,222 to 2,236 $\mu\text{mol kg}^{-1}$ at a



320 **Figure 8:** (a) Time series of raw pH in each station. (b) An example of detailed raw pH time series. Data in Shizugawa Bay from 2 to 9 February 2021 are presented here. (c) Time series of pH_{\min} in each station. Legends of colour plots are the same for all panels as shown in Fig. 8(c). The X-axis is expressed as year in decimal.



325 salinity of 33.5, which is approximately equal to that in the surface
waters of the western North Pacific in the corresponding latitudinal
range (Takatani et al., 2014). This phenomenon indicates that
coastal waters in these three areas are occasionally not significantly
modulated from their open water sources when salinity is
satisfactorily high (~33.5). In contrast, in Hinase and Ohno, we
330 we extended their regression equation to a salinity of 34.0. These
values again fit with those of Kuroshio waters (Takatani et al.,
2014), reflecting the fact that the ultimate source water for the Seto
Inland Sea is the Kuroshio. It is noteworthy that the maximum
salinity values observed in Hinase and Ohno were 31.67 and 31.43,
335 respectively (Fig. 7(b)). These results indicate that the open waters
of the Hinase and Ohno areas are already diluted from their
ultimate source (i.e., Kuroshio water), and hence, have already
received several modulations by coastal processes within the Seto
Inland Sea.

340 The freshwater endmember in each regression line
represents the Talk of the main freshwater source in each area,
although the absence of a low-salinity data point leads to a high
uncertainty in estimating the endmember. Table 1 describes the list
of Talk at the mouth of the major freshwater inflow in each coastal
345 area. By comparing these values with the freshwater endmember
calculated from Fig. 9, we can speculate which river was the actual major freshwater source for each area. For the Miyako
station, which is located at the northern edge of Miyako Bay, the Tashiro River becomes a major controller of salinity because
of its proximity to the station. Two small rivers are neighbouring the Kashiwazaki site, and both rivers can act as salinity
controllers for this site based on Talk. Interestingly, all small rivers that flow into Shizugawa Bay had far higher Talk values
350 than the calculated freshwater endmember, reflecting the existence of limestone areas in their basin. Rather, the Talk of
Kitakami River, despite flowing into a different bay south of Shizugawa, fitted with that of the freshwater endmember,
suggesting that this river is the main source of freshwater for Station S3 because of its large flow rate. In the Hinase Archipelago,
all surrounding rivers had similar Talk values, and hence, we cannot determine which rivers are the main freshwater sources
for Station H2. The freshwater endmember calculated in Ohno Strait was significantly higher than Talk of its neighbouring
355 large river (Ohta River), suggesting an additional contribution from small rivers directly facing this strait.

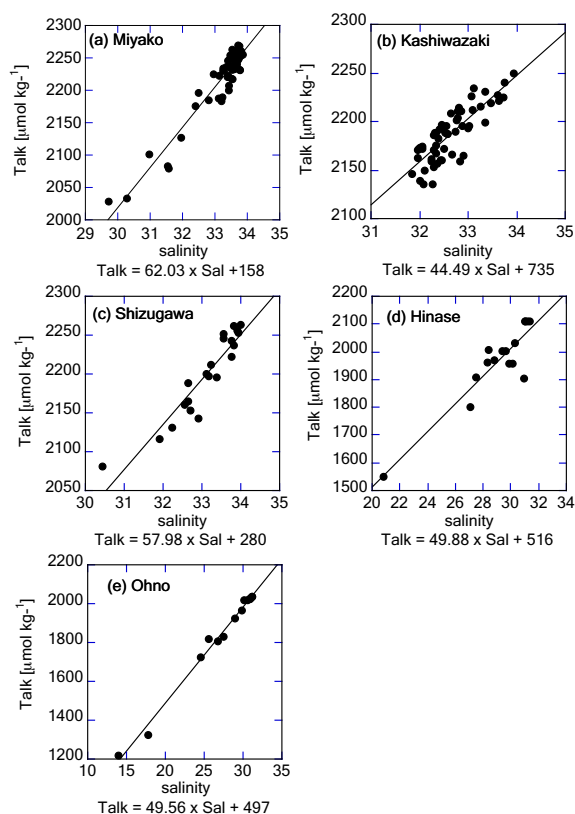


Figure 9: Salinity–Talk relationship based on discrete water samples obtained from (a) Miyako, (b) Kashiwazaki, (c) Shizugawa, (d) Hinase, and (e) Ohno stations. Regression equations are provided below the X-axes.



Table 1. Talk of freshwater sources in each coastal area, with calculated Talk of freshwater endmember from the salinity–Talk relationship (Fig. 9).

Area	Freshwater endmember of Talk from Fig. 9	Freshwater source in each area	Talk in each freshwater source
360 Miyako Bay	158±84 $\mu\text{mol kg}^{-1}$	Hei River	415 $\mu\text{mol kg}^{-1}$ ^a
		Tsugaruishi River	482 $\mu\text{mol kg}^{-1}$ ^b
		Tashiro River	142 $\mu\text{mol kg}^{-1}$ ^b
365 Kashiwazaki Coast	735±132 $\mu\text{mol kg}^{-1}$	Sabaishi River	845 $\mu\text{mol kg}^{-1}$ ^b
		Ukawa River	655 $\mu\text{mol kg}^{-1}$ ^b
Shizugawa Bay	280±172 $\mu\text{mol kg}^{-1}$	Kitakami River	351 $\mu\text{mol kg}^{-1}$ ^a
		Small rivers in Shizugawa Bay	725–1108 $\mu\text{mol kg}^{-1}$ ^b
370 Hinase Archipelago	516±169 $\mu\text{mol kg}^{-1}$	Chikusa River	525 $\mu\text{mol kg}^{-1}$ ^a
		Small rivers in the Archipelago	495–640 $\mu\text{mol kg}^{-1}$ ^b
Ohno Strait	497±36 $\mu\text{mol kg}^{-1}$	Ohta River	291 $\mu\text{mol kg}^{-1}$ ^a

375 a: values referred from Kobayashi (1960)
 b: measured in this study

3.4 Temporal variation of parameters derived from pH_{min} and Talk

Based on the regression equation obtained from Fig. 9, we calculated the time series of Talk from the time series of salinity at each station (Fig. 10(a)). We then calculated the time series of DIC, pCO_2 , Ω_{ara} , and Ω_{cal} from pH_{min} and Talk, and here, we show the results of pCO_2 and Ω_{ara} in Fig. 10(b) and Fig. 10(c).

As Talk was calculated as a linear equation of salinity, it is natural that the Talk time series resembles that of salinity (Fig. 10(a)). Sporadic decreases in Talk corresponding to low salinity events in Hinase and Ohno were noticeable. Water with low Talk has low buffer capacity, and hence, it has particularly high risks of low pH and high pCO_2 . Figure 10(b) shows an appearance of such risk, extremely high pCO_2 over 1,500 μatm during the low salinity period in Hinase and Ohno. The annually averaged pCO_2 values were 404, 450, 393, 589, and 621 μatm for Miyako, Kashiwazaki, Shizugawa, Hinase, and Ohno, respectively, showing that Hinase and Ohno were totally oversaturated with CO_2 , indicating extraordinarily high pCO_2 at low salinity events. Generally, estuary areas tend to become sources of atmospheric CO_2 , while “open” coastal areas such as marginal seas, continental shelves, and large bays tend to become sinks of atmospheric CO_2 (e.g., Borges et al., 2005; Laruelle et al., 2010; Kubo et al., 2017; Tokoro et al., 2020). Typically, terrestrial input of organic matter from rivers is mostly

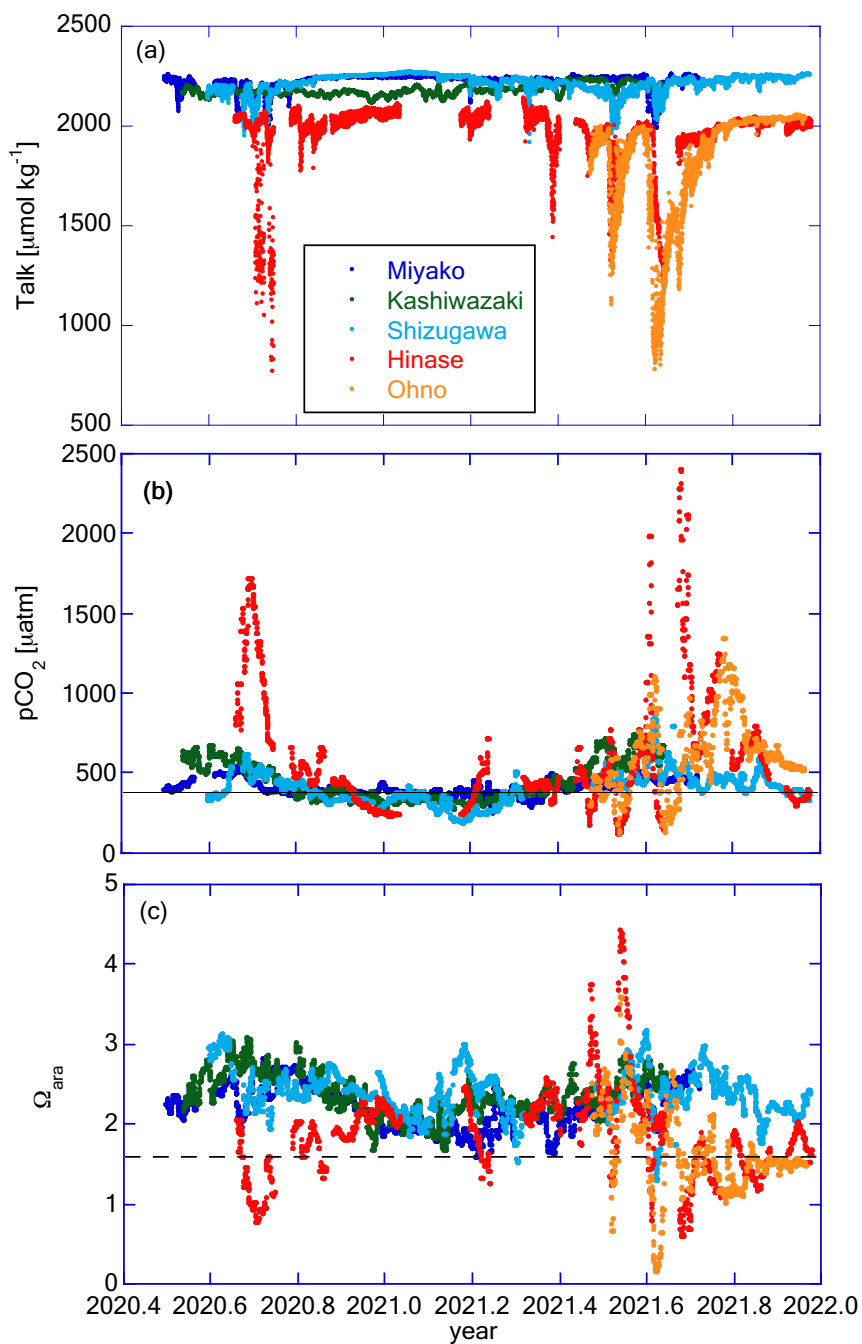


Figure 10: Time series of (a) Talk, (b) $p\text{CO}_2$, and (c) Ω_{ara} in the five stations. Legends of colour plots are the same for all panels as shown in Fig. 10(a). In all the graphs, the X-axis is expressed as year in decimal. Solid line in Fig. 10(b) represents the $p\text{CO}_2$ value in equilibrium with the present atmospheric CO_2 concentration of $400 \mu\text{atm}$. Dashed line in Fig. 10(c) represents the experimentally obtained threshold of the ocean acidification effect for the larvae of Pacific oyster *Crassostrea gigas* ($\Omega_{\text{ara}} = 1.5$, Waldbusser et al. [2015]).

395



decomposed in estuaries, causing high pCO₂ and low pH, as well as a high nutrient flux to the outer estuary. In an “open” coastal area, nutrients transported from the estuary activate high primary production, which causes low pCO₂ and high pH in surface waters. The Seto Inland Sea itself is considered a sink of atmospheric CO₂ (e.g., Tokoro et al., 2020), and hence, it can be treated as an open coastal area. Our result indicates that despite the high distance from the large river mouth, both Hinase Archipelago and Ohno Strait can be classified as “estuaries,” or at least as areas that receive a significant quantity of particulate organic matter from land.

Ω_{ara} was high in summer and low in winter in Miyako, Kashiwazaki, and Shizugawa (Fig. 10(c)), showing an opposite pattern to the seasonal variation of pH_{min}. This was due to the high seasonal variation in the solubility of aragonite induced by the seasonal change in water temperature (see Section 4.2). In contrast, in Hinase and Ohno, the amplitude of seasonal variation of pH was high enough to overcome seasonal variation of aragonite solubility, and as a result, Ω_{ara} changed to show a seasonal maximum in winter and a seasonal minimum in summer. Short-term variation of Ω_{ara} linked to that of salinity also overlapped this seasonal scale variation, and as a result, significantly low Ω_{ara} conditions were frequently observed in Hinase and Ohno. Fujii et al. (2023) described that during summer–autumn in the Hinase Archipelago, Ω_{ara} occasionally falls below the threshold level of the larvae of the Pacific oyster *Crassostrea gigas*, with the effect of ocean acidification (OA) becoming detectable in the rearing experiment ($\sim\Omega_{\text{ara}} = 1.5$; Waldbusser et al., 2015). This study showed that the situation was almost the same in Ohno Strait (Fig. 10(c)). It should be noted that Fujii et al. (2023) also noted that actual damaged larvae were not detected based on microscopic inspection of Hinase (n = 1062). The rearing experiment of Waldbusser et al. [2015] was conducted on the Oregon coast, where *C. gigas* is non-native. Therefore, it is not unrealistic that there is a difference in the tolerance for OA between the local population of Oregon and Seto Inland Sea, the latter being the native habitat of *C. gigas*. Kurihara et al. (2007) examined the effect of low pH in the Seto Inland Sea population of *C. gigas*, and found that the larvae of this population are affected by OA at a pH of 7.4 (National Bureau of Standards [NBS] scale). This threshold approximately corresponds to a pH of 7.27 in the total scale, and in this case, larvae of Pacific oysters are considered to be the same in most seasons both in Hinase and Ohno (Fig. 8(c)). In the experiment by Kurihara (2007), the rearing experiment was occupied only at the control (pH of 8.2 in the NBS scale) and acidified (pH of 7.4 in the NBS scale) conditions, and hence, true threshold for the Seto Inland Sea Pacific oyster population can exist between a pH of 7.27 and 8.07. We thus need further studies, including new rearing experiments, to determine why Pacific oyster larvae are still safe in the present Hinase Archipelago.

A low Ω_{ara} level below 1.6 was also detected in Shizugawa Bay (Fujii et al., 2023; see also Table 2 and Fig. 10(c) in this study), and Miyako Bay (Table 2 and Fig. 10(c)), but its duration was only four days and one day, respectively, throughout the study period. In Kashiwazaki, Ω_{ara} was above this level throughout the observation period. Other calcifiers are important for fisheries around the Japanese coast, such as Ezo abalone (*Haliotis discus hannai*) and short-spined sea urchin (*Strongylocentrotus intermedius*), have lower Ω_{ara} thresholds than that of Pacific oyster, 1.1 (Onitsuka et al., 2018) for *H. discus hannai* and 1.12 (Zhan et al., 2016) for *S. intermedius*. Therefore, Shizugawa Bay, Miyako Bay, and the Kashiwazaki Coast have a low risk of OA, at least from the viewpoint of fisheries. We, however, should note that we have investigated only



430 a few marine species so far, and there may be many unknown species that are vulnerable to low pH/low Ω_{ara} condition. We must enhance our knowledge of biological responses according to species, especially for those with low economic importance, such that we can evaluate the total risk posed by OA to the coastal ecosystem.

4 Discussion

435 4.1 Quantification of short-term variability in properties of water

We focused on short-term variations of pH and related parameters with timescales shorter than one month, which cannot be detected by regular MOE monitoring based on water sampling. To assess this quantitatively, we calculated the SD of each parameter at different timescales (annual, monthly, and 10-days), and the results are listed in Table 2. As shown in Figures 7 and 9, both the amplitude and frequency of short-term variation differed significantly among the seasons for almost all parameters. To determine seasonal differences in the extent of short-term variation, the monthly average of 10-days SD ($\overline{\text{SD}}^{\text{m}_{10}}$) was further calculated and is listed in Table 3.

Annual averages of monthly SD ($\overline{\text{SD}}^{\text{a}_{\text{m}}}$) of water temperature (0.9–1.5) were < 25% of the annual SD (3.9–7.2). The annual average of 10-days SD ($\overline{\text{SD}}^{\text{a}_{10}}$, 0.5–0.8) was approximately half of $\overline{\text{SD}}^{\text{a}_{\text{m}}}$ in each area (Table 2). Although the $\overline{\text{SD}}^{\text{m}_{10}}$ of water temperature varied seasonally (Table 3), it did not exceed the annual SD, even in the month with the annual maximum (Table 2). These phenomena indicate that seasonal scale variation is the main component of temporal variation for this property, and short-term variation is relatively lower than the seasonal variation (Fig. 7(a)).

In the case of salinity, the contribution of short-term variation to annual variability was higher than that of water temperature. The $\overline{\text{SD}}^{\text{a}_{\text{m}}}$ of salinity (0.33–2.37) was approximately half of the annual SD (0.66–5.34) in each area, and $\overline{\text{SD}}^{\text{a}_{10}}$ (0.26–1.40) was approximately two thirds of $\overline{\text{SD}}^{\text{a}_{\text{m}}}$. Seasonal variability of $\overline{\text{SD}}^{\text{m}_{10}}$ was also higher than that of water temperature (Table 3), and as a result, $\overline{\text{SD}}^{\text{m}_{10}}$ of salinity occasionally exceeded the annual SD in several months. This phenomenon indicates that the main component of the temporal variation of salinity is not seasonal scale variation but short-term variation (Fig. 7(b)). Interestingly, $\overline{\text{SD}}^{\text{a}_{10}}$ and $\overline{\text{SD}}^{\text{a}_{\text{m}}}$ were almost the same in Miyako, Kashiwazaki, and Shizugawa (Table 2), and the annual maximum of the 10-days SD for salinity was higher than that of the monthly SD. Such a phenomenon can be interpreted as caused by the perturbation of salinity that mainly occurs within the timescale of 10-days, and monthly SD of salinity is essentially determined by the amplitude and frequency of 10-days salinity variation included within that month. Although the $\overline{\text{SD}}^{\text{a}_{10}}$ of salinity was lower than $\overline{\text{SD}}^{\text{a}_{\text{m}}}$ in Hinase and Ohno, the annual maximum of SD of 10-days salinity was still higher than that of SD of monthly salinity, indicating that the 10-days variation is also an influential component of monthly variation in these two areas.

The relative contribution of short-term variation to annual variability for other parameters varied between the above two extremes (water temperature and salinity). In the case of DO, $\overline{\text{SD}}^{\text{a}_{\text{m}}}$ (9–22) was < half of the annual SD (26–60) in



Table 2. Statistical aspects of environmental parameters in each station.

Area	Miyako	Kashiwa-zaki	Shizu-gawa	Hinase	Ohno
465					
Water temp. [°C]					
1-year SD	4.9	7.2	5.6	6.6	3.9
monthly SD/annual avg. (\overline{SD}^a_m)	0.9	1.2	1.3	1.5	1.3
monthly SD /annual max.	2.1	2.2	2.2	2.7	2.1
470 10-day SD /annual avg. (\overline{SD}^a_{10})	0.5	0.6	0.6	0.6	0.8
10-day SD /annual max.	1.5	1.9	2.3	1.9	2.1
Salinity					
1-year SD	0.66	0.63	0.79	2.44	5.34
475 \overline{SD}^a_m	0.33	0.37	0.43	1.28	2.37
monthly SD /annual max.	1.10	0.64	1.04	5.67	7.47
\overline{SD}^a_{10}	0.26	0.25	0.37	0.81	1.40
10-day SD /annual max.	1.31	0.73	1.71	6.00	7.93
480					
Oxygen [$\mu\text{mol/kg}$]					
1-year SD	60	51	26	53	44
\overline{SD}^a_m	17	13	13	36	35
monthly SD /annual max.	28	20	22	62	57
\overline{SD}^a_{10}	9	7	10	11	22
485 10-day SD /annual max.	22	17	21	40	48
pH _{min}					
1-year SD	0.05	0.09	0.09	0.21	0.16
\overline{SD}^a_m	0.02	0.03	0.05	0.10	0.09
490 monthly SD /annual max.	0.06	0.05	0.09	0.23	0.24
\overline{SD}^a_{10}	0.02	0.02	0.03	0.06	0.07
10-day SD /annual max.	0.06	0.04	0.10	0.26	0.31
Ω_{ara}					
495 1-year SD	0.25	0.26	0.29	0.58	0.52
\overline{SD}^a_m	0.12	0.14	0.23	0.31	0.31
monthly SD /annual max.	0.21	0.22	0.48	0.89	0.78
\overline{SD}^a_{10}	0.09	0.11	0.15	0.22	0.25
500 10-day SD /annual max.	0.25	0.21	0.63	1.27	0.81

Numbers are shown in bold when they exceed the 1-year SD value.



Table 3. Monthly average of 10-day standard variation ($SD^{m_{10}}$) for each parameter on each month in each station. Numbers shown by bold represent annual maximum and the second maximum

Area	Parameter	Jan.	Feb.	Mar.	Apr.	May	Jun.	Jul.	Aug.	Sept.	Oct.	Nov.	Dec.	
Miyako	Water Temp. [°C]	0.26	0.17	0.15	0.28	0.64	0.72	0.86	0.58	0.70	0.53	0.35	0.45	
	Salinity	0.03	0.12	0.28	0.17	0.15	0.10	0.32	0.71	0.78	0.29	0.08	0.05	
	oxygen [$\mu\text{mol}/\text{kg}$]	8.9	13.1	10.8	14.4	13.5	8.4	9.5	6.0	7.3	5.2	3.3	5.6	
	pH	0.01	0.02	0.03	0.03	0.03	0.02	0.01	0.01	0.01	0.01	0.01	0.01	0.01
	Gara	0.03	0.08	0.11	0.14	0.12	0.14	0.08	0.13	0.13	0.07	0.04	0.04	
Kashiwazaki	Water Temp. [°C]	0.70	0.76	0.34	0.34	0.51	0.55	0.61	0.57	0.58	0.74	0.59	1.08	
	Salinity	0.25	0.41	0.20	0.20	0.38	0.15	0.37	0.20	0.13	0.21	0.18	0.30	
	oxygen [$\mu\text{mol}/\text{kg}$]	9.9	11.7	5.0	4.2	6.1	6.9	5.3	3.8	4.1	6.0	5.8	10.8	
	pH	0.02	0.02	0.02	0.02	0.02	0.03	0.02	0.02	0.02	0.02	0.02	0.03	
	Gara	0.08	0.13	0.09	0.08	0.10	0.08	0.13	0.12	0.10	0.12	0.11	0.15	
Shizugawa	Water Temp. [°C]	0.30	0.32	0.23	0.61	0.94	1.15	0.68	1.13	0.61	0.46	0.44	0.40	
	Salinity	0.04	0.13	0.32	0.58	0.56	0.32	0.77	0.61	0.66	0.23	0.18	0.09	
	oxygen [$\mu\text{mol}/\text{kg}$]	--	--	--	--	16.8	10.1	9.0	13.3	7.4	7.0	5.6	9.1	
	pH	0.02	0.04	0.03	0.04	0.03	0.02	0.03	0.03	0.05	0.03	0.02	0.02	0.01
	Gara	0.10	0.18	0.17	0.18	0.15	0.14	0.18	0.27	0.16	0.20	0.13	0.06	
Hinase	Water Temp. [°C]	0.88	--	0.51	0.41	0.60	0.34	0.71	1.00	0.49	0.71	0.65	0.72	
	Salinity	0.05	--	0.19	0.20	0.61	1.33	2.41	2.17	1.16	0.40	0.28	0.10	
	oxygen [$\mu\text{mol}/\text{kg}$]	--	--	--	--	--	--	--	--	16.4	13.1	8.2	7.5	
	pH	0.01	--	0.06	--	0.02	0.09	0.12	0.15	0.08	0.04	0.03	0.02	
	Gara	0.07	--	0.19	--	0.11	0.38	0.58	0.34	0.20	0.14	0.10	0.09	
Ohno	Water Temp. [°C]	--	--	--	--	--	1.26	0.90	1.13	0.61	0.54	0.49	0.44	
	Salinity	--	--	--	--	--	0.68	2.75	3.60	2.03	0.44	0.22	0.10	
	oxygen [$\mu\text{mol}/\text{kg}$]	--	--	--	--	--	17.9	29.6	31.0	29.3	29.7	9.5	4.6	
	pH	--	--	--	--	--	0.04	0.09	0.14	0.10	0.07	0.02	0.01	
	Gara	--	--	--	--	--	0.26	0.46	0.47	0.27	0.18	0.07	0.04	
Tokyo Bay*	Water Temp. [°C]	0.36	0.31	0.55	0.45	0.56	0.76	0.84	0.96	0.82	0.57	0.28	0.51	
	Salinity	0.34	0.35	0.79	0.72	0.67	1.35	2.11	1.65	1.41	0.86	0.53	0.46	
	pH	0.02	0.04	0.05	0.07	0.08	0.15	0.15	0.13	0.13	0.08	0.04	0.02	

*See Section 4.3 for the detail of the data in Tokyo Bay



all areas, but > 25% in Hinase and Ohno. The annual maximum of monthly SD exceeded annual SD in Hinase and Ohno. In
505 Ohno, even the annual maximum of 10-days SD exceeded annual SD (Table 2). These phenomena indicate that although the
main driver of the temporal variation of DO is water temperature, other drivers, such as biological processes, also contribute
to the short-term variation of DO. In the cases of pH_{\min} and Ω_{ara} , $\overline{\text{SD}}^{\text{a}}_{\text{m}}$ (0.02–0.10 and 0.12–0.31 for pH_{\min} and Ω_{ara} ,
respectively) was approximately half of the annual SD (0.05–0.21 and 0.25–0.58 for pH_{\min} and Ω_{ara} , respectively), and $\overline{\text{SD}}^{\text{a}}_{10}$
(0.02–0.07 and 0.09–0.25 for pH_{\min} and Ω_{ara} , respectively) was approximately one third of $\overline{\text{SD}}^{\text{a}}_{\text{m}}$. The annual maximum of both
510 the monthly SD and 10-days SD exceeded the annual SD in most areas. These phenomena indicate that short-term variation
in the 10-days scale is the main driver of annual temporal variation for both pH_{\min} and Ω_{ara} , which was similar to the case of
salinity.

We further investigated the seasonal dependency of the 10-days SD in each area based on Table 3. The annual
maximum of $\overline{\text{SD}}^{\text{m}}_{10}$ for DO, pH_{\min} , and Ω_{ara} occurred at approximately the same time, indicating the 10-days variations of these
515 three parameters were caused by the same processes (biological activities). However, the specific timing of the occurrence of
the annual maximum for these three parameters differed among the areas. In Miyako, the maximum $\overline{\text{SD}}^{\text{m}}_{10}$ for DO, pH_{\min} , and
 Ω_{ara} occurred in spring, when biological activities are the highest. In Shizugawa, Hinase, and Ohno, the maximum $\overline{\text{SD}}^{\text{m}}_{10}$ for
these parameters occurred during late summer and early autumn, which approximately overlapped with the timing of the
occurrence of the annual maximum of $\overline{\text{SD}}^{\text{m}}_{10}$ of salinity (Table 3). In Kashiwazaki, the maximum $\overline{\text{SD}}^{\text{m}}_{10}$ for DO, pH_{\min} , and
520 Ω_{ara} occurred in winter, when strong perturbation of river flow induced by heavy snowfall caused an annual maximum $\overline{\text{SD}}^{\text{m}}_{10}$
for both salinity and water temperature. Overall, the investigated statistical aspects of short-term variations indicated that
several physical processes related to the 10-days salinity variation had derivatively induced biological processes that caused
short-term variations in DO, pH_{\min} , and Ω_{ara} in these coastal areas.

4.2 Classification of temporal variations into thermodynamic and non-thermodynamic components

525 To determine the processes that contribute to the short-term variation in biogeochemical properties, we divided the
observed temporal variations of each property into thermodynamic and non-thermodynamic components using the following
equation:

$$C_i = C_i(\text{eq}) + C_i(\text{diseq}) \quad (1)$$

530

where C_i represents the observed concentration of parameter i , while $C_i(\text{eq})$ represents the estimated concentration of parameter
 i in equilibrium with the current atmosphere under the observed water temperature and salinity. $C_i(\text{diseq})$ represents the
difference between C_i and $C_i(\text{eq})$. For DO, $\text{DO}(\text{eq})$ was calculated from water temperature and salinity based on the formulation
of Weiss (1970) with a fixed atmospheric pressure of 1 atm. Both $\text{pH}(\text{eq})$ and $\Omega_{\text{ara}}(\text{eq})$ were calculated using the CO2sys



535 Table 4. Statistical aspects of thermodynamic and non-thermodynamic components.

Area	Miyako	Kashiwa- zaki	Shizu- gawa	Hinase	Ohno
540 DO(eq) [$\mu\text{mol/kg}$]					
1-year SD	33	40	27	35	20
monthly SD /annual avg.	6	7	13	8	6
monthly SD /annual max.	13	19	24	14	9
10-day SD /annual avg.	3	4	5	4	4
545 10-day SD /annual max.	10	8	7	5	6
DO(diseq) [$\mu\text{mol/kg}$]					
1-year SD	25	14	25	25	40
monthly SD /annual avg.	12	8	13	15	27
monthly SD /annual max.	22	17	21	28	48
550 10-day SD /annual avg.	8	4	11	11	23
10-day SD /annual max.	20	6	18	17	34
pH _{min} (eq)					
1-year SD	0.005	0.004	0.005	0.014	0.037
monthly SD /annual avg.	0.003	0.002	0.003	0.008	0.016
555 monthly SD /annual max.	0.008	0.004	0.007	0.034	0.057
10-day SD /annual avg.	0.002	0.001	0.002	0.004	0.009
10-day SD /annual max.	0.010	0.003	0.004	0.012	0.029
pH _{min} (diseq)					
1-year SD	0.051	0.093	0.114	0.210	0.158
560 monthly SD /annual avg.	0.024	0.031	0.049	0.103	0.090
monthly SD /annual max.	0.059	0.050	0.092	0.253	0.225
10-day SD /annual avg.	0.016	0.021	0.029	0.063	0.067
10-day SD /annual max.	0.103	0.028	0.048	0.156	0.124
Ω_{ara} (eq)					
565 1-year SD	0.4	0.6	0.4	0.5	0.5
monthly SD /annual avg.	0.1	0.1	0.1	0.2	0.3
monthly SD /annual max.	0.2	0.2	0.3	0.8	0.9
10-day SD /annual avg.	0.1	0.1	0.1	0.1	0.2
10-day SD /annual max.	0.2	0.1	0.1	0.3	0.4
570 Ω_{ara} (diseq)					
1-year SD	0.2	0.4	0.4	0.8	0.5
monthly SD /annual avg.	0.1	0.1	0.2	0.4	0.3
monthly SD /annual max.	0.2	0.2	0.4	0.9	0.7
10-day SD /annual avg.	0.1	0.1	0.1	0.2	0.2
575 10-day SD /annual max.	0.2	0.1	0.2	0.6	0.4

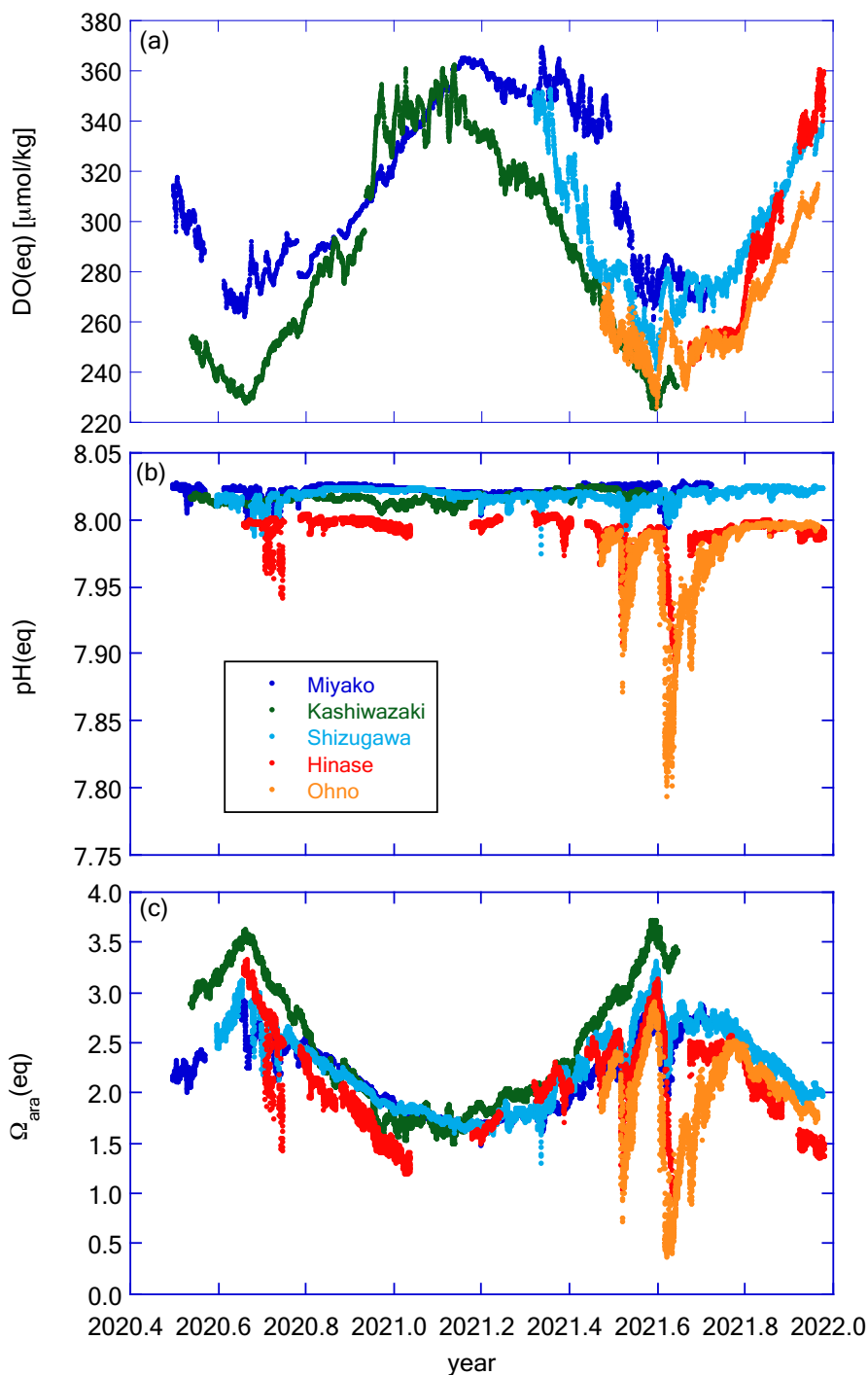
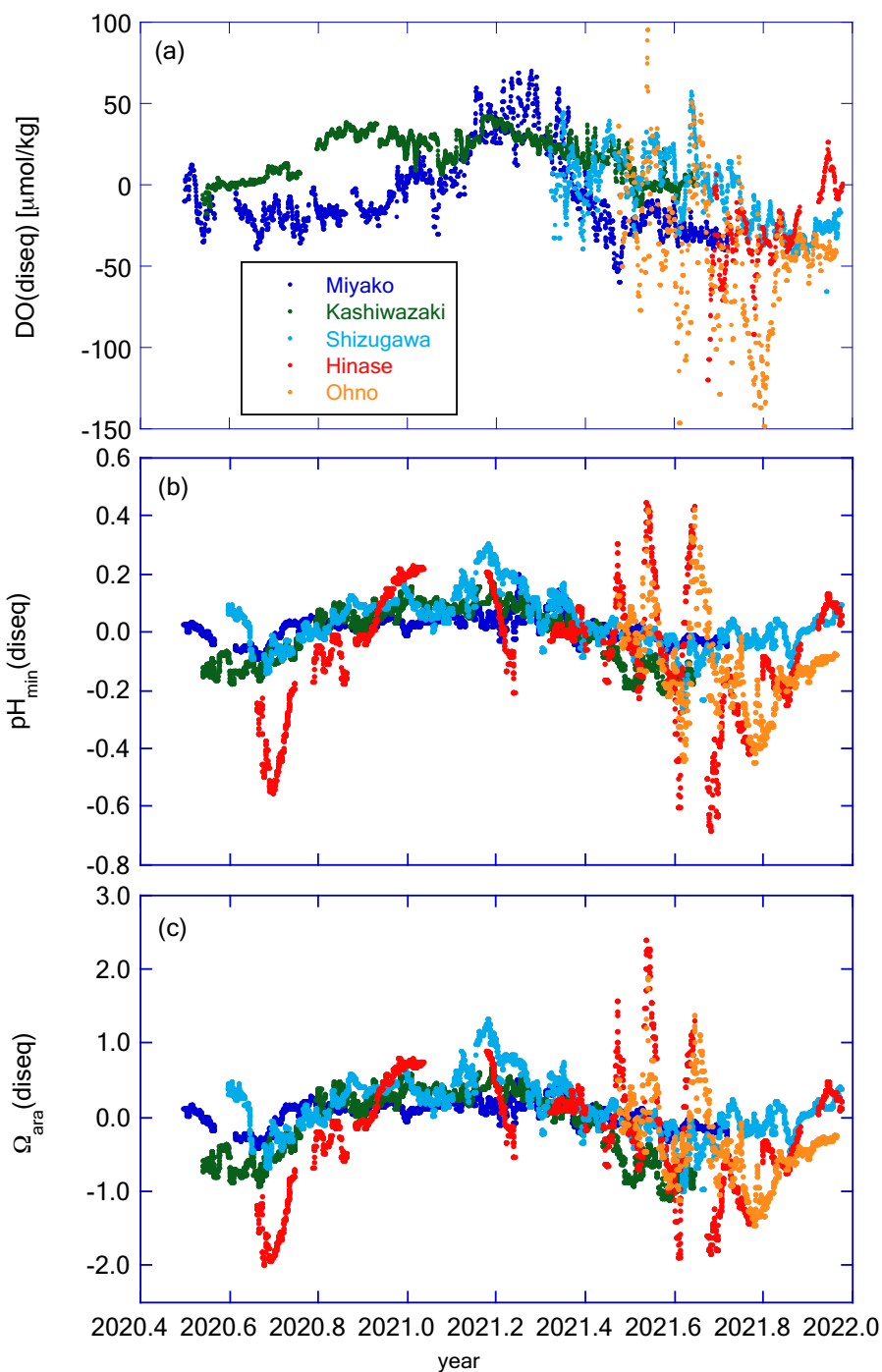


Figure 11: Time series of (a) DO(eq), (b) pH(eq), and (c) Ω_{ara} (eq) in the five stations. Legends of colour plots are the same for all panels as shown in Fig. 11(b). In all graphs, the X-axis is expressed as year in decimal.



580

Figure 12: Time series of (a) $\text{DO}(\text{diseq})$, (b) $\text{pH}_{\min}(\text{diseq})$, and (c) $\Omega_{\text{ara}}(\text{diseq})$ in the five stations. Legends of colour plots are the same for all panels as shown in Fig. 12(a). In all graphs, the X-axis is expressed as year in decimal.



program with the same set of constants as described in Section 2.1, using water temperature, salinity, estimated Talk, and a fixed atmospheric CO₂ mol fraction of 415 ppm.

585 Figure 11 shows the temporal variation of DO(eq), pH(eq), and $\Omega_{\text{ara}}(\text{eq})$, while Fig. 12 shows DO(diseq), pH_{min}(diseq), and $\Omega_{\text{ara}}(\text{diseq})$. We also calculated 1-year SD, monthly SD, and 10-days SD for these parameters, and the results are listed in Table 4.

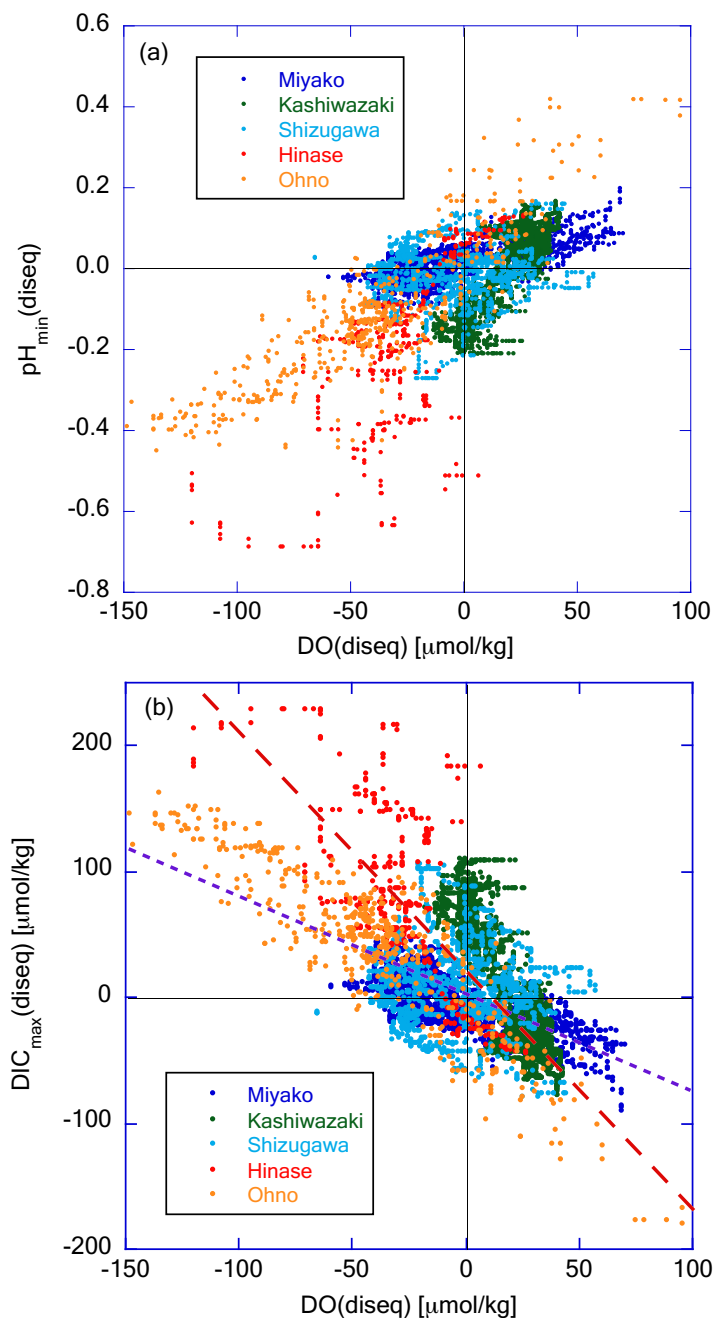
The annual temporal variation was approximately the same between DO(eq) and DO(diseq) (Table 4), but their origin was significantly different. While seasonal variation played a dominant role in the temporal variation of DO(eq) (Fig. 11(a), Table 4), short-term variations played a significant role in that of DO(diseq) (Fig. 12(a), Table 4). In the case of pH, the temporal variation of pH(eq) resembles that of salinity (Figs. 7(b) and 11(b)), and the amplitude of pH(eq) (~0.25, Fig. 11(b)) was approximately one order lower than that of pH(diseq) (~1.2, Fig. 12(b)). This result indicated that the thermodynamic process had a negligible contribution to the temporal variation of pH. Interestingly, the relative contributions of monthly SD and 10-days SD of pH(diseq) to the 1-year SD showed a similar structure to that of pH_{min} (Table 4), suggesting that the short-term variation at the scale of 10-days was the main driver of annual temporal variation for pH_{min}(diseq), which is similar to the cases of pH_{min} and salinity. Temporal variation of $\Omega_{\text{ara}}(\text{eq})$ had both seasonal- and short-term scale components (Table 4), and the pattern of seasonal variation resembled that of water temperature, while that of short-term variation resembled that of salinity (Fig. 11(c)). $\Omega_{\text{ara}}(\text{diseq})$ showed a similar scale of 1-year variability to that of $\Omega_{\text{ara}}(\text{eq})$ (Fig. 11(c) and Fig. 12(c), Table 4), similar to the case of DO. The temporal pattern of $\Omega_{\text{ara}}(\text{diseq})$ was quite similar to that of pH_{min}(diseq), suggesting that short-term variation at the 10-days scale contributes significantly to the annual temporal variation of $\Omega_{\text{ara}}(\text{diseq})$, similar to the case of pH_{min}(diseq). Overall, the non-thermodynamic component contributed approximately half of the observed annual variation in DO and Ω_{ara} , and in the case of pH, the non-thermodynamic component played a dominant role in the annual variation. For all these biogeochemical parameters, the short-term variation at the 10-days scale contributed a significant percentage of the temporal variation of the non-thermodynamic component.

605 To determine the specific process that drives the non-thermodynamic temporal variation of these properties, we examined the correlation between pH_{min}(diseq) and DO(diseq) (Fig. 13(a)). These two properties showed an approximately positive correlation, indicating that the non-thermodynamic component of temporal variations was driven mainly by biological processes. Several studies have also detected a positive relationship between variations in oxygen saturation and the metabolic component of pH in coastal waters, suggesting the primary influence of biological processes on pH dynamics (e.g., Baumann and Smith, 2018; Lowe et al., 2019). We further investigated the correlation between DIC_{min}(diseq) and DO(diseq) (Fig. 13(b)); the former was calculated as pH_{min}(diseq) and $\Omega_{\text{ara}}(\text{diseq})$. Most data obtained in Miyako and Ohno and approximately 50% of data obtained in Shizugawa approximately followed a linear regression line with the slope of $-\Delta\text{DIC}_{\text{min}}(\text{diseq})/\Delta\text{DO}(\text{diseq}) = 0.77$ (~106/138) crossing the origin, suggesting that the observed temporal variations of both DIC_{min}(diseq) and DO(diseq) were induced by the production/decomposition of planktonic oceanic particles in these two areas. The other data obtained in Shizugawa, as well as most data obtained in Hinase and Kashiwazaki followed the regression lines with steeper slopes than

615



that of open ocean stoichiometry. The respiratory quotients of estuarine ecosystems can occasionally be as high as 1.5 (Wang et al., 2018) or even 2.0 (Giblin et al., 1997), when affected by the anaerobic respiration process in estuarine sediments.



620 **Figure 13:** Plot of (a) $\text{pH}_{\text{min}}(\text{diseq})$ and (b) $\text{DIC}_{\text{max}}(\text{diseq})$ against $\text{DO}(\text{diseq})$, respectively. The purple dashed line in Fig. 13(b) represents the theoretical line when assuming that biological production / degradation of organic matter occur with the Redfield relationship ($-\Delta \text{pH}_{\text{min}}(\text{diseq}) / \Delta \text{DO}(\text{diseq}) = 106/138$). The red dashed line represents the regression line of Hinase data.



The observed high $-\Delta\text{DIC}_{\text{min}}(\text{diseq})/\Delta\text{DO}(\text{diseq})$ ratio thus suggests that lateral affection of biological processes in the neighbouring estuaries contributes significantly to the observed temporal variations of $\text{DIC}_{\text{min}}(\text{diseq})$ and $\text{DO}(\text{diseq})$ in these three areas.

625 4.3 Controlling factor of the amplitude of short-term pH variation.

The analysis clearly shows that severe low pH/low Ω_{ara} situations occur only at the short-term pH drawdown events that coincide with rainfall events in the coastal areas of Japan (Fig. 9(c) and 10(c)). As the amplitude of pH variation related to rainfall events differed among the five coastal areas, it is important to understand the controlling factor that determines the amplitude of short-term pH variation. To investigate this issue, we analysed the relationship of statistical short-term
 630 variabilities between salinity and pH_{min} . Since short-term variation mainly occurred in the timescale of < 10 days for both salinity and pH_{min} (see discussion in Section 4.1), we plotted the $\overline{\text{SD}}_{10}^{\text{m}}$ of pH_{min} against that of salinity (Fig. 14). In this analysis, we introduced continuous monitoring data of pH and salinity obtained in Tokyo Bay (off Kawasaki Artificial Island, <https://www.tbeic.go.jp/MonitoringPost/manual/aboutObservedPoint02.pdf>) to obtain information on highly eutrophicated coastal areas. The details of the observation methods and the location settings of this station are described in the Appendix.

635

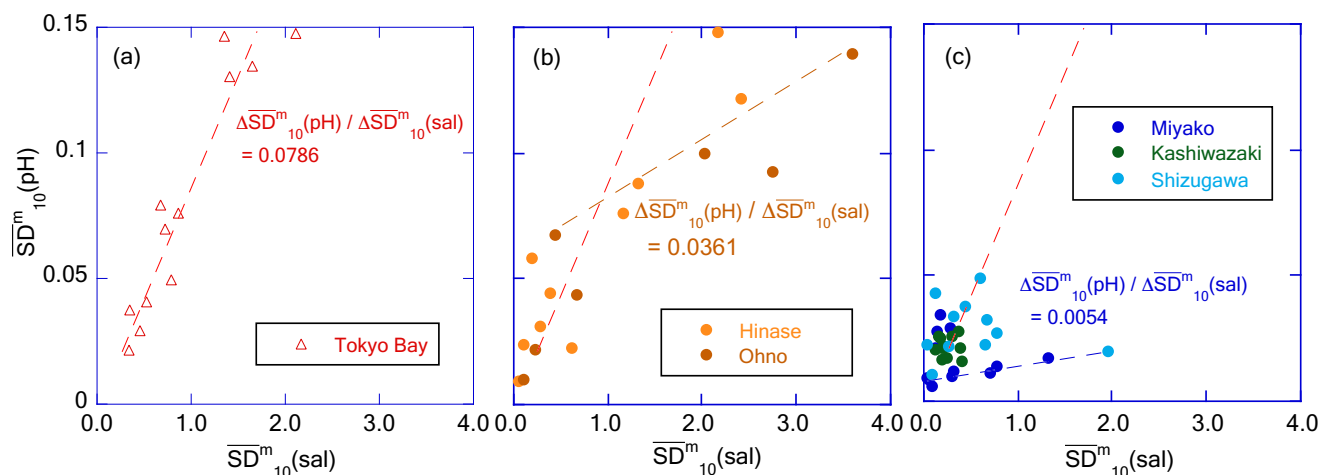


Figure 14: Plots of $\overline{\text{SD}}_{10}^{\text{m}}(\text{pH})$ against $\overline{\text{SD}}_{10}^{\text{m}}(\text{sal})$ for (a) Tokyo Bay, (b) Hinase and Ohno, and (c) Miyako, Kashiwazaki, and Shizugawa, respectively. The red, brown, and blue dashed lines represents the regression lines of Tokyo Bay, Hinase and Ohno, and Miyako, Kashiwazaki, and Shizugawa, respectively.

640

In Tokyo Bay, $\overline{\text{SD}}_{10}^{\text{m}}$ of pH_{min} (hereafter $\overline{\text{SD}}_{10}^{\text{m}}(\text{pH})$) linearly increased with an increase in $\overline{\text{SD}}_{10}^{\text{m}}$ of salinity ($\overline{\text{SD}}_{10}^{\text{m}}(\text{sal})$, Fig. 14(a)), suggesting that freshwater transports the sources of biological processes (both organic carbon and dissolved nutrients) at a constant concentration regardless of the flow rate. On the other hand, In Hinase and Ohno, $\overline{\text{SD}}_{10}^{\text{m}}(\text{pH})$



increased with that of $\overline{SD}^{m}_{10}(\text{sal})$ at the same rate as observed in Tokyo Bay when $\overline{SD}^{m}_{10}(\text{sal})$ was low, but $\Delta\overline{SD}^{m}_{10}(\text{pH}) /$
645 $\Delta\overline{SD}^{m}_{10}(\text{sal})$ changed to a low value when $\overline{SD}^{m}_{10}(\text{sal})$ exceeded 1.0 (Fig. 14(b)). This phenomenon indicated that the
concentration of biologically active materials transported by freshwater into the Seto Inland Sea was diluted at a high
freshwater flow rate, while it was not diluted in the rivers flowing into Tokyo Bay, as the latter receives far higher
anthropogenic loadings from its drainage basin than the dose received by the Seto Inland Sea. In the coastal area receiving
further low anthropogenic loadings such as Miyako, Kashiwazaki, and Shizugawa, $\Delta\overline{SD}^{m}_{10}(\text{pH}) / \Delta\overline{SD}^{m}_{10}(\text{sal})$ was much lower
650 than that of Hinase and Ohno when $\overline{SD}^{m}_{10}(\text{sal})$ exceeded 1.0 (Fig. 14(c)).

We cited the nutrient concentration of the main freshwater sources for each of the three coastal area categories (i.e.,
Tashiro, Sabaishi, and Kitakami Rivers for Miyako + Kashiwazaki + Shizugawa, Chikusa and Ohta Rivers for Hinase + Ohno,
Ara, Tama, and Tsurumi Rivers for Tokyo Bay, respectively) from the MOE Public Water Quality Database, and calculated
the weighted mean nitrate concentration ($\overline{NO_3}$) of river waters that flow into each coastal area using water transport as the
655 weight. We then found that $\Delta\overline{SD}^{m}_{10}(\text{pH}) / \Delta\overline{SD}^{m}_{10}(\text{sal})$ observed at high freshwater input (that is, $\overline{SD}^{m}_{10}(\text{sal}) > 1.0$) showed a
linear relationship with $\overline{NO_3}$ in each coastal area category (Fig. 15). This result implies that the amplitude of short-term

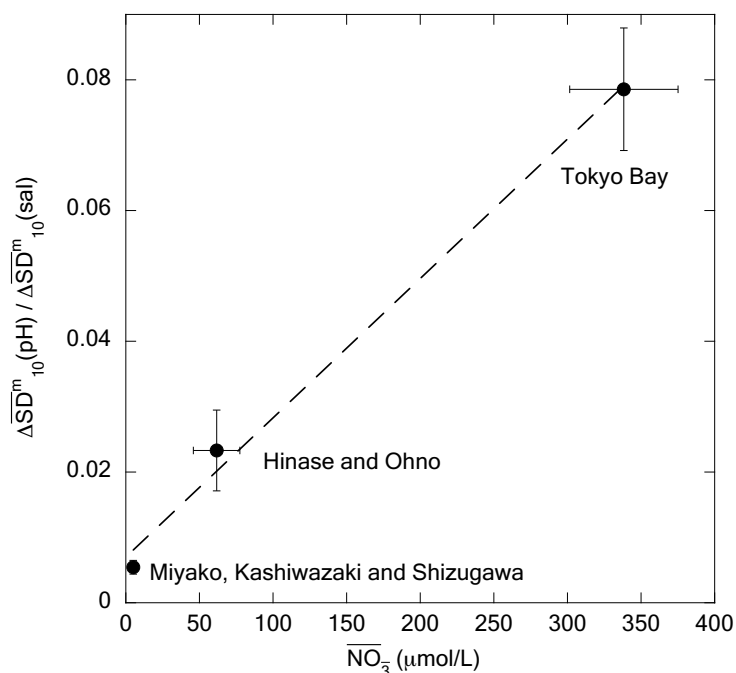


Figure 15: Plot of $\Delta\overline{SD}^{m}_{10}(\text{pH}) / \Delta\overline{SD}^{m}_{10}(\text{sal})$ against $\overline{NO_3}$ for each coastal
area category. The dashed line represents the regression line.

variation of pH_{min} in coastal areas is principally
determined by the quantity of nutrients
transported by freshwater from the hinterland.
660 We, however, need to note that the riverine
nitrate concentration can be an implicit function
of other controlling factors. For example, the
quantity of suspended organic particles in river
waters, as well as accumulated organic
665 materials in riverine and estuarine sediments
should be linearly correlated with the riverine
nitrate concentration, and hence, the $\overline{NO_3}$ in
Fig. 15 may actually be an indicator of the
transport of these materials. We thus need
670 further detailed observations, especially at the
time of increase in water level of the river, to
understand practical processes that cause short-
term pH variation in coastal waters.



5 Conclusion

675 In this study, we synthesised data from continuous pH monitoring of five coastal areas in Japan from 2020 to 2021. Annual variability (~ 1 SD) of pH and Ω_{ara} were 0.05–0.09 and 0.25–0.29, respectively, for three areas with low anthropogenic loadings (Miyako Bay, Kashiwazaki Coast, and Shizugawa Bay), while they increased to 0.16–0.21 and 0.52–0.58, respectively, in two areas with medium anthropogenic loadings (Hinase Archipelago and Ohno Strait in Seto Inland Sea). Statistical assessment of temporal variability at various timescales revealed that most of the annual variabilities in both pH and
680 Ω_{ara} were derived by short-term variation with a timescale of < 10 days, rather than the seasonal-scale variation. Our analyses further illustrated that most of the short-term pH variation (and hence, annual variation) was caused by biological processes, while both thermodynamic and biological processes equally contributed to the temporal variation in Ω_{ara} . Biological alteration of pH mainly occurred in oceanic areas in Miyako Bay and Ohno Strait, whereas it occurred mainly in estuarine areas in Kashiwazaki Coast and Hinase Archipelago. In Shizugawa Bay, both oceanic and estuarine areas were responsible for the
685 biological alteration of pH.

The observed results show that short-term acidification with Ω_{ara} of < 1.5 occurred occasionally in Miyako and Shizugawa Bays, while it occurred frequently in the Hinase Archipelago and Ohno Strait. Many such short-term acidified events were related to short-term low-salinity events. Our analyses showed that the amplitude of short-term pH variation was linearly correlated with that of short-term salinity variation, and its regression coefficient at the time of high freshwater input
690 was positively correlated with the nutrient concentration of the main river that flows into the coastal area.

Fortunately, no marine organism that has been damaged by ocean acidification has been detected in coastal areas of Japan. However, our study showed that Ω_{ara} in Japanese coastal areas occasionally drops to a level that is potentially hazardous for marine organisms, such as Pacific oysters (< 1.5 , Waldbusser et al., 2015) even in the present state. It is already known that the pH in Japanese coastal areas is decreasing at the same rate as that of the open ocean (Ishizu et al., 2019 and Ishida et al.,
695 2021), and hence, the extent, duration, and frequency of such short-term low pH and Ω_{ara} situations will increase in coastal areas in Japan in the future. Our study indicates that the amplitude of the short-term drawdown of pH related to low-salinity events will decrease if we can reduce the nutrient concentration of rivers, and this will contribute to suppressing the extent and duration of short-term low-salinity events in coastal areas in the future. We should note, however, that a certain percentage of Japanese coastal areas are now suffering due to the problem of low biological productivity derived from the decreased
700 anthropogenic nutrient input (e.g., Yamamoto et al., 2021). We must consider the balance between the risk of ocean acidification and oligotrophication when we control anthropogenic loadings to coastal waters in the future. We should also note that not only the concentration of dissolved nutrients, but also other biologically active materials such as suspended organic materials in river waters and accumulated organic materials in riverine and estuarine sediments may be responsible for short-term pH variations at low salinity events (e.g., Carstensen and Duarte, 2019). Our analysis revealed that seawaters in
705 both the Hinase Archipelago and Ohno Strait were oversaturated with CO_2 all through the years, and hence, it is considered



710 that more organic matter than that biologically produced within these areas was decomposed. In such cases, not only the reduction of dissolved nutrients but also the reduction of particulate organic matter transported from rivers to coastal areas will contribute to the suppression of short-term pH drawdown. Many studies have already mentioned the contribution of seaweed/seagrass beds to the effective capture of suspended organic sediments in estuaries (e.g., Potouroglou et al., 2017; Barcelona et al., 2021; Levia-Duenas et al., 2023), and hence, the conservation and/or development of seaweed/seagrass beds in estuarine and coastal areas will contribute to the reduction of organic matter transport from rivers to coastal areas at times of high river flow. To specify effective measures against the current coastal acidification in Japan, further detailed observations, especially at the time of increase in water level of the river, are needed such that we can obtain a detailed understanding of practical processes that cause short-term pH variation in coastal waters.

715 **6 Appendix: Observation methods and location settings of Tokyo Bay data**

Detailed data for Tokyo Bay (Kawasaki Artificial Island, Section 4.3), referred to by us, are described in the home page of data holders: <https://www.tbeic.go.jp/MonitoringPost/manual/aboutObservedPoint02.pdf>. Here, we provide a brief summary.

720 Kawasaki Artificial Island (KAI) is located in the centre of Tokyo Bay, the bay with the highest population in its basin area (2.9 million) and highest nutrient loadings (210 tN d^{-1}) in Japan (Fig. A1). KAI is a huge concrete cylinder with a diameter of 200 m, in which an air vending system for the trans-bay freeway tunnel is stored. An autonomous ocean profiling system was set off KAI, which included a YSI 6600V2-4M multiple ocean sensor for the measurement of water temperature, salinity, and pH. The mechanical measurement resolution of pH was ± 0.01 . The sensors were cleaned and calibrated on a monthly basis. Although the pH sensor was calibrated against NBS buffers, we used pH data without conversion to a total scale, as we
725 used these pH data only for the analysis of temporal variability. Vertical profiles were measured hourly, and the obtained data were distributed from the public database managed by the Tokyo Bay Environmental Information Center (<https://www.tbeic.go.jp/MonitoringPost/ViewGraph/ViewGraph?buoyId=02>). We downloaded KAI data pertaining to July 2020 to December 2021 from this database and used them for analysis.

7 Data Availability

730 Data from Tokyo Bay can be downloaded from the Tokyo Bay Environmental Information Center Public Database (<https://www.tbeic.go.jp/MonitoringPost/ViewGraph/ViewGraph?buoyId=02>). Other data used in this study are provided in the Supplementary Materials.



8 Author contribution

735 TO and DM performed field measurements and water sampling in Miyako Bay. MH and MY performed field measurements and water sampling on the Kashiwazaki Coast. AD performed field measurements and water sampling in Shizugawa Bay. SO, TT, MF, and RH performed field measurements and water samplings in the Hinase Archipelago. TO, GO, and KK performed field measurements and water sampling in Ohno Strait. TO undertook the measurements of discrete carbonate samples taken in Miyako Bay and Kashiwazaki Coast, while MW undertook the measurements of those taken in Shizugawa Bay, Hinase Archipelago, and Ohno Strait. Analyses of data obtained by these efforts were performed by TO.

740 9 Acknowledgements

We thank all fishers who helped us with their boats and offered their support for monitoring in Shizugawa Bay and the Hinase Archipelago. We also thank Dr. Yukihiro Nojiri, Dr. Hideaki Nakata, Dr. Osamu Matsuda, and Dr. Tetsuo Yanagi for their fruitful advice and discussions during our analyses. This study was funded both by the Ocean Acidification Adaptation Project (OAAP) of the Nippon Foundation and the Study of Biological Effects of Acidification and Hypoxia (BEACH) of the 745 Environment Research and Technology Development Fund Grant Number JPMEERF20202007 of the Environmental Restoration and Conservation Agency of Japan.

10 References

- Abo, K. and Onitsuka, G.: Characteristics of currents induced by heavy rainfall in Hiroshima Bay in July 2018, Proceedings of the Japan Society of Civil Engineers, Ser. B, 75, 1051-1056, in Japanese, 2019.
- 750 Barcelona, A., Oldham, C., Colomer, J., Garcia-Orellana, J., and Serra, T.: Particle capture by seagrass canopies under an oscillatory flow, Coastal Engineering, 169, 103972, <https://doi.org/10.1016/j.coastaleng.2021.103972>, 2021.
- Barton, A., Hales, B., Waldbusser, G. G., Langdon, C. and Feely, R. A.: The Pacific oyster, *Crassostrea gigas*, shows negative correlation to naturally elevated carbon dioxide levels: Implications for near-term ocean acidification effects, Limnology and Oceanography, 57, 698-710, <https://doi.org/10.4319/lo.2012.57.3.0698>, 2012.
- 755 Bates, N. R., Astor, Y. M., Church, M. J., Currie, K., Dore, J. E., González-Dávila, M., Lorenzoni, L., Muller-Karger, F., Olafsson, J. and Santana-Casiano, J. M.: A time-series view of changing surface ocean chemistry due to ocean uptake of anthropogenic CO₂ and ocean acidification, Oceanography, 27, 126-141, <https://doi.org/10.5670/oceanog.2014.16>, 2014.
- Baumann, H. and Smith, E. M.: Quantifying metabolically driven pH and oxygen fluctuations in US nearshore habitats at diel to interannual timescales, Estuaries and Coasts, 41, 1102-1117, <https://doi.org/10.1007/s12237-017-0321-3>, 2018.
- 760 Bernardo, L. P. C., Fujii, M., and Ono, T.: Development of a high-resolution marine ecosystem model for predicting the combined impacts of ocean acidification and hypoxia, Frontiers in Marine Science, Submit, 2023.



- Booth, J. A. T., McPhee-Shaw, E. E., Chua, P., Kingsley, E., Denny, M., Phillips, R., Bograd, S. J., Zeidberg, L. D. and Gilly, W. F.: Natural intrusions of hypoxic, low pH water into nearshore marine environments on the California coast, *Continental Shelf Research*, 45, 108-115, <https://doi.org/10.1016/j.csr.2012.06.009>, 2012.
- 765 Borges, A. V., Delille, B., and Frankignoulle, M.: Budgeting sinks and sources of CO₂ in the coastal ocean: Diversity of ecosystems counts, *Geophysical Research Letters*, 32, L14601, <https://doi.org/10.1029/2005GL023053>, 2005.
- Borges, A. V. and Gypens, N.: Carbonate chemistry in the coastal zone responds more strongly to eutrophication than to ocean acidification, *Limnology and Oceanography*, 55, 346-353, 2010.
- Cai, W.-J., Hu, X., Huang, W.-J., Murrell, M. C., Lehrter, J. C., Lohrenz, S. E., Chou, W.-C., Zhai, W., Hollibaugh, J. T.,
770 Wang, Y., Zhao, P., Guo, X., Gundersen, K., Dai, M., and Gong, G.-C.: Acidification of subsurface coastal waters enhanced by eutrophication, *Nature Geoscience*, 4, 1297, <https://doi.org/10.1038/ngeo1297>, 2011.
- Cai, W.-J., Huang, W.-J., Luther III, G. W., Pierrot, D., Li, M., Testa, J., Xue, M., Joesoef, A., Mann, R., Brodeur, J., Xu, Y.-Y., Chen, B., Waldbusser, G. G., Cornwell, J. and Kemp, W. M.: Redox reactions and weak buffering capacity lead to acidification in the Chesapeake Bay, *Nature Communications*, 8, 369, <https://doi.org/10.1038/s41467-017-00417-7>, 2017.
- 775 Carstensen, J. and Duarte, C. M.: Drivers of pH variability in coastal ecosystems, *Environmental Science and Technology*, 53, 4020-4029, <https://doi.org/10.1021/acs.est.8b03655>, 2019.
- Christian, J. and Ono, T.: Ocean acidification and deoxygenation in the North Pacific Ocean, North Pacific Marine Science Organization, Sidney, 116 pp., 2019.
- Delille, B., Borges, A. V. and Delille, D.: Influence of giant kelp beds (*Macrocystis pyrifera*) on diel cycles of pCO₂ and DIC
780 in the Sub-Antarctic coastal area, *Estuarine, Coastal and Shelf Science*, 81, 114-122, <https://doi.org/10.1016/j.ecss.2008.10.004>, 2009.
- Dickson, A. G.: Standard potential of the reaction: AgCl(s) + 12H₂ (g) = Ag(s) + HCl(aq), and the standard acidity constant of the ion HSO₄⁻ in synthetic sea water from 273.15 to 318.15 K, *The Journal of Chemical Thermodynamics*, 22, 113-127, [https://doi.org/10.1016/0021-9614\(90\)90074-Z](https://doi.org/10.1016/0021-9614(90)90074-Z), 1990.
- 785 Duarte, C. M., Hendriks, I. E., Moore, T. S., Olsen, Y. S., Steckbauer, A., Ramajo, L., Carstensen, J., Trotter, J. A., and McCulloch, M.: Is ocean acidification an open-ocean syndrome? Understanding anthropogenic impacts on seawater pH, *Estuaries and Coasts*, 36, 221-236, <https://doi.org/10.1007/s12237-013-9594-3>, 2013.
- Feely, R. A., Alin, S. R., Carter, B., Bednarsek, N., Hales, B., Chan, F., Hill, T. M., Gaylord, B., Sanford, E., Byrne, R. H., Sabine, C. L., Greeley, D. and Juranek, L.: Chemical and biological impacts of ocean acidification along the west coast of
790 North America, *Estuarine, Coastal and Shelf Science*, 183, 260-270, <https://doi.org/10.1016/j.ecss.2016.08.043>, 2016.
- Feely, R. A., Sabine, C. L., Hernandez-Ayon, J. M., Ianson, D. and Hales, B.: Evidence for upwelling of corrosive “acidified” water onto the continental shelf, *Science*, 320, 1490e1492, <https://doi.org/10.1126/science.1155676>, 2008.
- Fujii, M., Hamanoue, R., Bernardo, L. P., Ono, T., Dazai, A., Oomoto, S., Katao, S., Wakita, M., and Tanaka, T.: Observed and projected impacts of coastal warming, acidification and deoxygenation on Pacific oyster (*Crassostrea gigas*) farming:



- 795 Case studies in the Hinase Area, Okayama Prefecture and Shizugawa Bay, Miyagi Prefecture, Japan, *Biogeoscience*, submit, 2023.
- Fujii, M., Takao, S., Yamaka, T., Akamatsu, T., Fujita, Y., Wakita, M., Yamamoto, A., and Ono, T.: Continuous monitoring and future projection of ocean warming, acidification, and deoxygenation on the subarctic coast of Hokkaido, Japan, *Frontiers in Marine Science*, 8, 590020, <https://doi.org/10.3389/fmars.2021.590020>, 2021.
- 800 Giblin, A. E., Hopkinson, C. S. and Tucker, J.: Benthic metabolism and nutrient cycling in Boston Harbor, *Estuaries, Mountains, Estuaries*, 20, 346-364, <https://doi.org/10.2307/1352349>, 1997.
- Gomez, F. A., Wanninkhof, R., Barbero, L. and Lee, S.-K.: Increasing river alkalinity slows ocean acidification in the northern Gulf of Mexico, *Geophysical Research Letters*, 48, e2021GL096521, <https://doi.org/10.1029/2021GL096521>, 2021.
- Guo, X., Yao, Z., Gao, Y., Luo, Y., Xu, Y., and Zhai, W.: Seasonal variability and future projection of ocean acidification on the East China Sea shelf off the Changjiang Estuary, *Frontiers in Marine Science*, 8, 770034, <https://doi.org/10.3389/fmars.2021.770034>, 2021.
- 805 Hauri, C., Gruber, N., Vogt, M., Doney, S. C., Feely, R. A., Lachkar, Z., Leinweber, A., McDonnell, A. M. P., Munnich, M. and Plattner, G.-K.: Spatiotemporal variability and long-term trends of ocean acidification in the California Current System, *Biogeosciences*, 10, 193-216, <https://doi.org/10.5194/bg-10-193-2013>, 2013.
- 810 Higashi, H., Sato, Y., Yoshinari, H., Maki, H., Koshikawa, H., Kanaya, G. and Uchiyama, Y.: Freshwater discharge from small river basins and its impacts on reproductivity of coastal hydrodynamic simulation in Seto Inland Sea, *Proceedings of the Japan Society of Civil Engineers, Ser. B*, 74, 1135-11140, in Japanese, 2018.
- Hoshiba, Y., Hasumi, H., Itoh, S., Matsumura, Y. and Nakada, S.: Biogeochemical impacts of flooding discharge with high suspended sediment on coastal seas: A modelling study for a microtidal open bay, *Scientific Reports*, 11, 21322, <https://doi.org/10.1038/s41598-021-00633-8>, 2021.
- 815 Iida, Y., Takatani, Y., Kojima, A. and Ishii, M.: Global trends of ocean CO₂ sink and ocean acidification: an observation-based reconstruction of surface ocean inorganic carbon variables, *Journal of Oceanography*, 77, 323-358, <https://doi.org/10.1007/s10872-020-00571-5>, 2021.
- Ishida, H., Isono, R. S., Kita, J. and Watanabe, Y. W.: Long-term ocean acidification trends in coastal waters around Japan, *Nature Scientific Reports*, 11, 5052, <https://doi.org/10.1038/s41598-021-84657-0>, 2021.
- 820 Ishizu, M., Miyazawa, Y., Tsunoda, T., and Ono, T.: Long-term trends in pH in Japanese coastal seawater, *Biogeosciences*, 16, 4747-4763, <https://doi.org/10.5194/bg-16-4747-2019>, 2019.
- Jiang, L.-Q., Carter, B. R., Feely, R. A., Lauvset, S. K. and Olsen, A.: Surface ocean pH and buffer capacity: past, present and future, *Nature Scientific Report*, 9, 18624, <https://doi.org/10.1038/s41598-019-55039-4>, 2019.
- 825 Johnson, Z. I., Wheeler, B. J., Blinebry, S. K., Carlson, C. M., Ward, C. S. and Hunt, D. E.: Dramatic variability of the carbonate system at a temperate coastal ocean site (Beaufort, North Carolina, USA) is regulated by physical and biogeochemical processes on multiple timescales, *PLoS ONE*, 8, e85117, <https://doi.org/10.1371/journal.pone.0085117>, 2013.



- 830 Kakehi, S., Naiki, K., Kodama, T., Wagawa, T., Kuroda, H., and Ito, S.-I.: Projections of nutrient supply to a wakame (*Undaria pinnatifida*) seaweed farm on the Sanriku Coast of Japan, *Fisheries Oceanography*, 27, 323-335, <https://doi.org/10.1111/fog.12255>, 2018.
- Kessouri, F., McWilliams, J. C., Bianchi, D., Sutula, M., Renault, L., Deutsch, C., Feely, R. A., McLaughlin, K., Ho, M., Howard, E. M., Bednars̆ek, N., Damien, P., Molemaker, J. and Weisberg, S. B.: Coastal eutrophication drives acidification, oxygen loss, and ecosystem change in a major oceanic upwelling system, *Proceedings of the National Academy of Sciences*, 118, e2018856118, <https://doi.org/10.1073/pnas.2018856118>, 2021.
- 835 Ko, Y. H., Lee, K., Noh, J. H., Lee, C. M., Kleypas, J. A., Jeong, H. J. and Kim, K. Y.: Influence of ambient water intrusion on coral reef acidification in the Chuuk Lagoon, located in the coral-rich western Pacific Ocean, *Geophysical Research Letters*, 43, 3830-3838, <https://doi.org/10.1002/2016GL068234>, 2016.
- Kobayashi, J.: Study on average water quality of Japanese rivers and its features, *Studies in Agriculture*, 48, 63-104, in Japanese, 1960.
- 840 Kubo, A., Maeda, Y., and Kanda, J.: A significant net sink for CO₂ in Tokyo Bay, *Nature Scientific Reports*, 7, 44355, <https://doi.org/10.1038/srep44355>, 2017.
- Kurihara, H., Kato, S. and Ishimatsu, A.: Effects of increased seawater pCO₂ on early development of the oyster *Crassostrea gigas*, *Aquatic Biology*, 1, 91-98, 2007.
- Laruelle, G. G., Dürr, H. H., Slomp, C. P. and Borges, A. V.: Evaluation of sinks and sources of CO₂ in the global coastal ocean using a spatially explicit typology of estuaries and continental shelves, *Geophysical Research Letters*, 37, L15607, <https://doi.org/10.1029/2010GL043691>, 2010.
- 845 Lauvset, S. K., Gruber, N., Landschützer, P., Olsen, A. and Tjiputra, J.: Trends and drivers in global surface ocean pH over the past three decades, *Biogeoscience*, 12, 1285-1298, <https://doi.org/10.5194/bg-12-1285-2015>, 2015.
- Lee, K., Kim, T.-W., Bryne, R. H., Millero, F. J., Feely, R. A. and Liu, Y.-M.: The universal ratio of boron to chlorinity for the North Pacific and North Atlantic oceans, *Geochimica et Cosmochimica Acta*, 74, 1801-1811, <https://doi.org/10.1016/j.gca.2009.12.027>, 2010.
- 850 Leiva-Dueñas, C., Graversen, A. E. L., Banta, G. T., Holmer, M., Masque, P., Stæhr, P. A. U. and Krause-Jensen, D.: Capturing of organic carbon and nitrogen in eelgrass sediments of southern Scandinavia, *Limnology and Oceanography*, online first, <https://doi.org/10.1002/lno.12299>, 2023.
- 855 Lewis, E. and Wallace, D. W. R.: Program developed for CO₂ system calculations, Carbon Dioxide Information Analysis Center, ORNL/CDIAC 105, 38 pp., 1998.
- Lowe, A. T., Bos, J., Ruesink, J.: Ecosystem metabolism drives pH variability and modulates long-term ocean acidification in the Northeast Pacific coastal ocean, *Nature Scientific Reports*, 9, 963, <https://doi.org/10.1038/s41598-018-37764-4>, 2019.
- 860 Lueker, T. J., Dickson, A. G. and Keeling, C. D.: Ocean pCO₂ calculated from dissolved inorganic carbon, alkalinity, and equations for K₁ and K₂: validation based on laboratory measurements of CO₂ in gas and seawater at equilibrium, *Marine*



- Chemistry, 70, 105-119, 2000. [https://doi.org/10.1016/S0304-4203\(00\)00022-0](https://doi.org/10.1016/S0304-4203(00)00022-0)
- Ministry of Environment, Japan: Public Water Quality Database, available at <https://water-pub.env.go.jp/water-pub/mizu-site/mizu/kousui/dataMap.asp> (last access: October 29 2022), 2022.
- Mongin, M., Baird, M. E., Tilbrook, B., Matear, R. J., Lenton, A., Herzfeld, M., Wild-Allen, K., Skerratt, J., Margvelashvili, N., Robson, B. J., Duarte, C. M., Gustafsson, M. S. M., Ralph, P. J. and Steven, A. D. L.: The exposure of the Great Barrier Reef to ocean acidification, *Nature Communications*, 7, 10732, <https://doi.org/10.1038/ncomms10732>, 2016.
- Niigata Prefectural Institution of Fisheries Oceanography: 1997 Annual report of ocean monitoring for ocean climate forecast for fisheries, 106 pp., in Japanese, 1998.
- Nishijima, W.: Management of nutrient concentrations in the Seto Inland Sea, *Bulletin on Coastal Oceanography*, 56, 13-19, in Japanese, 2018.
- Okada, T., Maruya, Y., Nakayama, K. and Iseri, E.: A study on restoration of eelgrass (*Zostera marina*) damaged by tsunami in Miyako Bay, *Proceedings of the Japan Society of Civil Engineers, Ser. B*, 70, 1186-1190, in Japanese, 2014.
- Onitsuka, T., Takami, H., Muraoka, D., Matsumoto, Y., Nakatsubo, A., Kimura, R., Ono, T., Nojiri, Y.: Effects of ocean acidification with pCO₂ diurnal fluctuations on survival and larval shell formation of Ezo abalone, *Haliotis discus hannai*, *Marine Environmental Research* 134, 28-36, <https://doi.org/10.1016/j.marenvres.2017.12.015>, 2018.
- Papalexioiu, S. M. and Montanari, A.: Global and regional increase of precipitation extremes under global warming, *Water Resources Research*, 55, 4901-4914, <https://doi.org/10.1029/2018WR024067>, 2019.
- Potouroglou, M., Bull, J. C., Krauss, K. W., Kennedy, H. A., Fusi, M., Daffonchio, D., Mangora, M. M., Githaiga, M. N., Diele, K., and Huxham, M.: Measuring the role of seagrasses in regulating sediment surface elevation, *Nature Scientific Reports*, 7, 11917, <https://doi.org/10.1038/s41598-017-12354-y>, 2017.
- Provoost, P., Heuven, S. v., Soetaert, K., Laane, R. W. P. M. and Middelburg, J. J.: Seasonal and long-term changes in pH in the Dutch coastal zone, *Biogeosciences*, 7, 3869-3878, <https://doi.org/10.5194/bg-7-3869-2010>, 2010.
- Ricart, A. M., Ward, M., Hill, T. M., Sanford, E., Kroeker, K. J., Takeshita, Y., Merolla, S., Shukla, P., Ninokawa, A. T., Elsmore, K. and Gaylord, B.: Coast-wide evidence of low pH amelioration by seagrass ecosystems, *Global Change Biology*, 27, 2580-2591, <https://doi.org/10.1111/gcb.15594>, 2021.
- Salisbury, J., Green, M., Hunt, C., and Campbell, J.: Coastal acidification by rivers: A threat to shellfish?, *EOS*, 89, 513-528, 2008. <https://doi.org/10.1029/2008EO500001>
- Salisbury, J. E. and Jönsson, B. F.: Rapid warming and salinity changes in the Gulf of Maine alter surface ocean carbonate parameters and hide ocean acidification, *Biogeochemistry*, 141, 401-418, <https://doi.org/10.1007/s10533-018-0505-3>, 2018.
- Sugimura, A., Takeda, A., Nihei, Y. and Ohtsuki, K.: Evaluation of sediment, nutrient and organic matter transport from a wide range of land to coastal ocean, *Proceedings of the Japan Society of Civil Engineers, Ser. B*, 71, 1423-1428, in Japanese, 2015.



- 895 Sunda, W. G. and Cai, W.-J.: Eutrophication induced CO₂-acidification of subsurface coastal waters: Interactive effects of
temperature, salinity, and atmospheric pCO₂, *Environmental Science and Technology*, 46, 10651-10659,
<https://doi.org/10.1021/es300626f> 2012.
- Takahashi, T., Sutherland, S. C., Chipman, D. W., Goddard, J. G., Ho, C., Newberger, T., Sweeney, C. and Munro, D. R.:
900 Climatological distributions of pH, pCO₂, total CO₂, alkalinity, and CaCO₃ saturation in the global surface ocean, and
temporal changes at selected locations, *Marine Chemistry*, 164, 95-125, <https://doi.org/10.1016/j.marchem.2014.06.004>,
2014.
- Takatani, Y., Enyo, K., Iida, Y., Kojima, A., Nakano, T., Sasano, D., Kosugi, N., Midorikawa, T., Suzuki, T. and Ishii, M.:
Relationships between total alkalinity in surface water and sea surface dynamic height in the Pacific Ocean, *Journal of
Geophysical Research*, 119, 2806-2814, <https://doi.org/10.1002/2013JC009739>, 2014.
- 905 Tokoro, T., Nakaoka, S.-i., Takao, S., Kuwae, T., Kubo, A., Endo, T. and Nojiri, Y.: Contribution of biological effects to
carbonate system variations and the air–water CO₂ flux in urbanised bays in Japan, *Journal of Geophysical Research*, 126,
e2020JC016974, <https://doi.org/10.1029/2020JC016974>, 2020.
- Tsukamoto, H. and Yanagi, T.: Temporal and Spatial variations in water temperature, salinity, pH, nutrient salts and
chlorophyll-a in the Seto Inland Sea, *Umi no Kenkyu*, 7, 11-19, in Japanese, 1998.
- Vargas, C. A., Contreras, P. Y., Pérez, C. A., Sobarzo, M., Saldías, G. S. and Salisbury, J.: Influences of riverine and upwelling
910 waters on the coastal carbonate system off Central Chile and their ocean acidification implications, *Journal of Geophysical
Research*, 121, 1468-1483, <https://doi.org/10.1002/2015JG003213>, 2015.
- Wakita, M., Sasaki, K., Nagano, A., Abe, H., Tanaka, T., Nagano, K., Sugie, K., Kaneko, H., Kimoto, K., Okunishi, T., Takada,
M., Yoshino, J. and Watanabe, S.: Rapid reduction of pH and CaCO₃ saturation state in the Tsugaru Strait by the intensified
Tsugaru Warm Current during 2012–2019, *Geophysical Research Letters*, 48, e2020GL091332,
915 <https://doi.org/10.1029/2020GL091332>, 2021.
- Waldbusser, G. G., Hales, B., Langdon, C. J., Haley, B. A., Schrader, P., Brunner, E. L., Gray, M. W., Miller, C. A. and
Gimenez, I.: Saturation-state sensitivity of marine bivalve larvae to ocean acidification, *Nature Climate Change*, 5, 273-
280, <https://doi.org/10.1038/NCLIMATE2479>, 2015.
- Waldbusser, G. G. and Salisbury, J. E.: Ocean acidification in the coastal zone from an organism's perspective: Multiple system
920 parameters, frequency domains, and habitats, *Annual Review of Marine Science*, 6, 221-47,
<https://doi.org/10.1146/annurev-marine-121211-172238>, 2014.
- Wallace, R. B., Baumann, H., Grear, J. S., Aller, R. C. and Gobler, C. J.: Coastal ocean acidification: The other eutrophication
problem, *Estuarine, Coastal and Shelf Science*, 148, 1-13, <https://doi.org/10.1016/j.ecss.2014.05.027>, 2014.
- 925 Wang, S. R., Iorio, D. D., Cai, W.-J. and Hopkinson, C. S.: Inorganic carbon and oxygen dynamics in a marsh-dominated
estuary, *Limnology and Oceanography*, 63, 47-71, <https://doi.org/10.1002/lno.10614>, 2018.
- Weiss, R. F.: The solubility of nitrogen, oxygen and argon in water and seawater, *Deep-Sea Research*, 17, 721-735, 1970.



- Yamamoto, H., Yoshiki, K., Komatsu, T., Sasa, S., Hayama, M., Murata, H. and Yanagi, T.: Numerical evaluation of environmental capacity of aquaculture in Shizugawa Bay - comparison before and after the Great East Japan Earthquake-, Proceedings of the Japan Society of Civil Engineers, Ser. B, 73, 1339-1344, 2017.
- 930 Yamamoto, H., Yoshiki, K., Komatsu, T., Sasa, S. and Yanagi, T.: Numerical evaluation of carrying capacity of aquaculture in Shizugawa Bay using land-sea integrated ecosystem model, Proceedings of the Japan Society of Civil Engineers, Ser. B, 74, 1279-1284, in Japanese, 2018.
- Yamamoto, T., Ishida, M. and Seiki, T.: Long-term variation in phosphorus and nitrogen concentrations in the Ohta River water, Hiroshima, Japan as a major factor causing the change in phytoplankton species composition Bulletin of Japan
935 Society of Fisheries Oceanography, 102-109, in Japanese, 2002.
- Yamamoto, T., Orimoto, K., Asaoka, S., Yamamoto, H. and Onodera, S.-i.: A Conflict between the legacy of eutrophication and cultural oligotrophication in Hiroshima Bay, Oceans, 2, 546-565, <https://doi.org/10.3390/oceans2030031>, 2021.
- Yamamoto-Kawai, M., Ito, S., Kurihara, H. and Kanda, J.: Ocean acidification state in the highly eutrophic Tokyo Bay, Japan: Controls on seasonal and interannual variability, Frontiers in Marine Sciences, 8, 642041,
940 <https://doi.org/10.3389/fmars.2021.642041>, 2021.
- Yanagi, T. and Ishii, D.: Open ocean originated phosphorus and nitrogen in the Seto Inland Sea, Japan, Journal of Oceanography, 60, 1001-1005, 2004.
- Yao, H., Wang, J., Han, Y., Jiang, X. and Chen, J.: Decadal acidification in a subtropical coastal area under chronic eutrophication, Environmental Pollution, 293, 118487, <https://doi.org/10.1016/j.envpol.2021.118487>, 2022.
- 945 Zhan, Y., Hu, W., Zhang, W., Liu, M., Duan, L., Huang, X., Chang, Y. and Li, C.: The impact of CO₂-driven ocean acidification on early development and calcification in the sea urchin *Strongylocentrotus intermedius*, Marine Pollution Bulletin, 112, 291-302, <https://doi.org/10.1016/j.marpolbul.2016.08.003>, 2016.